The Canadian Mineralogist
Vol. 37, pp. 731-762 (1999)

BORATE MINERALS. II. A HIERARCHY OF STRUCTURES BASED UPON THE BORATE FUNDAMENTAL BUILDING BLOCK

JOEL D. GRICE

Research Division, Canadian Museum of Nature, P.O. Box 3443, Station D, Ottawa, Ontario K1P 6P4, Canada

PETER C. BURNS

Department of Civil Engineering and Geological Sciences, University of Notre Dame, Notre Dame, Indiana 46556, U.S.A.

FRANK C. HAWTHORNE§

Department of Geological Sciences, University of Manitoba, Winnipeg, Manitoba R3T 2N2, Canada

Abstract

A hierarchical structural classification is developed for borate minerals, based on the linkage of (BO_3) triangles and (BO_4) tetrahedra to form *FBB*s (fundamental building blocks) that polymerize to form the structural unit, a tightly bonded anionic polyhedral array whose excess charge is balanced by the presence of large low-valence interstitial cations. Thirty-one minerals, with nineteen distinct structure-types, contain isolated borate polyhedra. Twenty-seven minerals, with twenty-five distinct structure-types, contain finite clusters of borate polyhedra. Ten minerals, with ten distinct structure-types, contain chains of borate polyhedra. Fifteen minerals, with thirteen distinct structure-types, contain sheets of borate polyhedra. Fifteen minerals, with thirteen distinct structure-types, contain frameworks of borate polyhedra. It is only the close-packed structures of the isolated-polyhedra class that show significant isotypism.

Keywords: borate minerals, crystal structures, structural hierarchy.

Sommaire

Nous développons ici un schéma de classification structurale des minéraux du groupe des borates, fondé sur l'articulation des triangles (BO_3) et des tétraèdres (BO_4), qui forment des modules structuraux fondamentaux. Ceux-ci, polymérisés, constituent l'unité structurale de la maille, un agencement compact d'anions fait de ces polyèdres dont l'excédent de charge est neutralisé par des cations interstitiels à rayon relativement gros et à valence relativement faible. Trente-et-un minéraux, classifiés en dix-neuf types structuraux, contiennent des polyèdres isolés de borate. Vingt-sept minéraux, dont vingt-cinq types structuraux, contiennent des agroupements limités de polyèdres de borate. Dix minéraux, dont dix types structuraux distincts, contiennent des chaînes de polyèdres de borate. Quinze minéraux, dont treize types structuraux, contiennent des feuillets de polyèdres de borate. Quinze minéraux, dont treize types structuraux, contiennent des trames de polyèdres de borate. Seules les structures à empilement compact de polyèdres isolés font preuve d'isotypisme important.

(Traduit par la Rédaction)

Keywords: borates, minéraux, structures cristallines, hiérarchie structurale.

Introduction

Boron is not a common element in the Earth's crust, but fractionation in crustal processes results in the concentration of boron and fascinatingly complex deposits of borate minerals. For example, Canada's most significant borate deposits, in the Penobsquis and Salt Springs marine evaporites in Sussex, New Brunswick, contain at least twenty borate species, four of which are not known from any other locality (Roulston & Waugh 1981, Rachlin *et al.* 1986, Mandarino *et al.* 1990, Burns *et al.* 1992, Roberts *et al.* 1993, Grice *et al.* 1994, 1996, 1997, Burns & Carpenter 1996). The deposit is even more significant because three of the four new minerals have structures with remarkable affinities to aluminosilicate zeolites (Grice *et al.* 1994, 1996). Such struc-

§ *E-mail address*: frank_hawthorne@umanitoba.ca

tural complexity can occur because the boron cation occurs both as ($B\phi_3$) triangles and ($B\phi_4$) tetrahedra (ϕ: O^{2-}, OH^-); the superscripts indicate the formal charges of anions and cations in the borate minerals. The polymerization of these two distinct types of coordination polyhedra results in exceptionally complex structures. The structures of over 100 borate minerals are now known; here, the structures are compared and arranged into a hierarchy of structures.

Boron–oxygen bonds are of much higher bond-valence than the interstitial bonds, and thus borate minerals are very suitable for hierarchical classification based on the topological character of the *FBB* (fundamental building block) and the structural unit. There have been several classifications or structural hierarchies of this sort proposed for the borate minerals. Early versions by Edwards & Ross (1960), Ross & Edwards (1967), Christ (1960), Tennyson (1963) and Heller (1970) were reviewed by Christ & Clark (1977), who also produced the scheme in general use until now. The recent solution of several complex borate structures, both minerals (Grice *et al.* 1994, 1996) and synthetic phases (Behm 1983, 1985, Heller & Pickardt 1985, Hotokka & Pyykkö 1989), prompted further development on the topological character of *FBB*s of the form $[B_n\phi_m]$ with $3 \le n \le 6$ (Burns *et al.* 1995). The hierarchy presented here is based on the set of *FBB*s and linkage nomenclature developed by Burns *et al.* (1995). The general philosophy follows that of Hawthorne (1985, 1986, 1990, 1994): the *FBB*, a cluster of coordination polyhedra with the strongest bond-valence linkages in the structure, is repeated (usually polymerized) to form the *structural unit*, a complex (usually) anionic array, the charge of which is balanced by the presence of large low-valence *interstitial* cations. Hierarchical ordering is a function of the topological character of the *FBB* and the dimensional and topological character of the polymerization of the *FBB* to form the structural unit.

Throughout this paper, the descriptor proposed by Burns *et al.* (1995) for borate clusters and *FBB*s is used. Each *FBB* has a descriptor of the form *A*:*B*, where *A* gives the number of borate triangles (Δ) and tetrahedra (□) in the *FBB* in the form *i*Δ*j*□, where *i* and *j* are the numbers of triangles and tetrahedra, respectively. The *B* part of the descriptor is a character string that contains information on the connectivity of the polyhedra. The string is written such that adjacent Δ or □ (or both) represent polyhedra that share corners, and the delimiters <> indicate that the included polyhedra share corners to form a ring. The sharing of polyhedra between rings is indicated by the symbols –, =, ≡, *etc.*, for one, two, three or more polyhedra, respectively. For example, the *FBB* with the descriptor 2Δ2□:<Δ2□>=<Δ2□> contains two triangles and two tetrahedra. There are two three-membered rings of polyhedra, each of which contains one triangle and two tetrahedra, and the rings have two tetrahedra in common. Further details are given by Burns *et al.* (1995).

Structures Based on Isolated Polyhedra

There are two possible *FBB*s in this class, Δ and □, and this class can be divided into two groups on this basis. Each of these groups can be divided into two subgroups according to the identity of the anions coordinating the central B, O^{2-} or $(OH)^-$, as this has important structural and paragenetic consequences. Minerals in this class are listed in Table 1.

FBB = 1Δ:Δ, $\phi = O^{2-}$; the 3Å wallpaper structures

These structures consist of infinite $[M\phi_4]$ chains of edge-sharing octahedra cross-linked by $T\phi_3$ triangles (T = B) and ($T\phi_4$) tetrahedra (T = S, Cr^{6+}, P, As^{5+}, V^{5+}, Si) (Hawthorne 1985, 1986, 1990). The $[M\phi_4]$ chain has an intrinsic repeat-distance of ~3 Å along its length. In the borates, the chains are cross-linked by $B\phi_3$ triangles in the plane perpendicular to the length of the chains, and by edges and vertices shared with adjacent chains. Ignoring ordering along the length of the chains, the graphical (topological) aspects of these structures may be idealized as colorings of the regular 3^6 net. These structures can be divided into two subsets, the zigzag structures and the miscellaneous structures.

The zigzag structures: Takéuchi *et al.* (1978) and Takéuchi (1978) introduced the idea of *F* walls, *C* walls and *S* columns to describe the structure of orthopinakiolite and its relation to the structure of pinakiolite. This description works very well for the structures of several other (commonly paragenetically) related borate minerals listed in Table 1. We call these minerals the *zigzag borates* because of the striking zigzag patterns that are apparent when these structures are viewed down their 3*n* Å axis.

The structures of these minerals are shown in Figure 1. There are three principal elements apparent in this view: (1) straight truncated chains of edge-sharing octahedra extending diagonally through the structures, (2) zigzag truncated chains of octahedra between the chains described in (1), and (3) (BO_3) triangles occupying interstices between the straight and zigzag chains (Fig. 1). Both sets of chains of octahedra share edges with similar chains that are displaced ~3 Å along [001] to form flat sheets and zigzag sheets, respectively. In orthopinakiolite, Takéuchi *et al.* (1978) called the flat sheet the *F* wall; the zigzag sheet was described as a *C* (corrugated) wall flanked by columns of octahedra designated as *S* columns. This notation is shown by the shading of polyhedron elements in Figure 1. Each *F* wall is terminated at each end by an *S* column. Similarly, each *C* wall is terminated at each end by sharing octahedron corners with an *S* column. Note that the terminal octahedra of each *F* wall also belong to the attached *C*-wall. There are equal numbers of octahedra in the *F* wall, the *C* wall and the *S* column, and hence we can write each structure as $F_nC_nS_n$, where *n* is the number of octahedra in each wall in the structure (note that when considering

TABLE 1. BORATE MINERALS BASED ON ISOLATED $B\Phi_3$ OR $B\Phi_4$ POLYHEDRA

Polyhedra	Name	Connectivity	Formula	*a* (Å)	*b* (Å)	*c* (Å)	α (°)	β (°)	γ (°)	Sp. Gr.	Ref.	Fig.
			3 Å wallpaper structures									
Zigzag borates												
1Δ	azoproite	Δ	$Mg_2(Fe^{3+},Ti^{4+},Mg)(BO_3)O_2$	9.26(1)	12.25(1)	3.01(1)	–	–	–	*Pbam*	(1)	–
1Δ	bonaccordite	Δ	$Ni_2Fe^{3+}(BO_3)O_2$	9.213(6)	12.229(7)	3.001(2)	–	–	–	*Pbam*	(2)	–
1Δ	fredrikssonite	Δ	$Mg_2Mn^{3+}(BO_3)O_2$	9.198(2)	12.528(3)	2.965(1)	–	–	–	*Pbam*	(3)	–
1Δ	ludwigite	Δ	$Mg_2Fe^{3+}(BO_3)O_2$	9.257(1)	12.282(1)	3.0234(2)	–	–	–	*Pbam*	(4)	1a
1Δv	vonsenite	Δ	$Fe^{2+}_2Fe^{3+}(BO_3)O_2$	9.463(1)	12.305(1)	3.073(1)	–	–	–	*Pbam*	(5)	–
1Δ	chestermanite***	Δ	$Mg_2(Fe^{3+},Mg,Al,Sb^{5+})(BO_3)O_2$	18.535(3)	12.273(1)	6.043(1)	–	–	–	*Pnnm*	(6)	–
1Δ	orthopinakiolite**	Δ	$Mn^{3+}_7(Mn^{2+},Mg,Fe^{3+},\square)_{17}(BO_3)_8O_{16}$	18.357(4)	12.591(2)	6.068(1)	–	–	–	*Pnnm*	(7)	1b
1Δ	takéuchiite**	Δ	$Mn^{3+}_{11}(Mn^{2+},Mg,Fe^{3+},\square)_{25}(BO_3)_{12}O_{24}$	27.585(4)	12.561(3)	6.027(2)	–	–	–	*Pnnm*	(8)	1c
1Δ	blatterite**	Δ	$Sb^{5+}_3Mn^{3+}_9(Mn^{2+},Mg)_{35}(BO_3)_{16}O_{32}$	37.654(8)	12.615(3)	6.2472(8)	–	–	–	*Pnnm*	(9)	1d
1Δ	'Mg-blatterite"*	Δ	$Sb^{5+}_3Mn^{3+}_9(Mg,Mn^{2+})_{35}(BO_3)_{16}O_{32}$	37.384(11)	12.568(3)	6.200(2)	–	–	–	*Pnnm*	(10)	–
1Δ	pinakiolite	Δ	$(Mg,Mn^{2+})_2(Mn^{3+},Sb^{3+})(BO_3)O_2$	21.79(1)	5.977(5)	5.341(5)	–	95.83(5)	–	*C2/m*	(11)	1e
Miscellaneous wallpaper borates												
1Δ	fluoborite	Δ	$Mg_3[BO_3](F,OH)_3$	8.827(3)	8.827(3)	3.085(2)	–	–	–	$P6_3/m$	(12)	2a
1Δ	painite	Δ	$CaZrAl_9O_{15}[BO_3]$	8.715(2)	8.715(2)	8.472(2)	–	–	–	$P6_3$	(13)	–
1Δ	jeremejevite	Δ	$Al_6[BO_3]_5F_3$	8.56	8.56	8.18	–	–	–	$P6_3/m$	(14)	–
1Δ	warwickite	Δ	$(Mg,Ti,Fe^{3+},Al)_3[BO_3]O$	9.246(1)	3.0927(2)	9.384(1)	–	–	–	*Pnma*	(15)	2b
1Δ	yuanfuliite	Δ	$Mg(Fe^{3+},Fe^{2+},Al,Ti,Mg)(BO_3)O$	9.258(6)	3.081(2)	9.351(4)	–	–	–	*Pnma*	(16)	–
1Δ	karlite	Δ	$Mg_7(OH)_4(BO_3)_3Cl$	17.637(1)	17.967(2)	3.1040(2)	–	–	–	$P2_12_12_1$	(19)	2c
1Δ	wightmanite	Δ	$Mg_5O(OH)_5[BO_3]$	13.46(2)	3.102(5)	18.17(2)	–	91.60(5)	–	*I2/m*	(20)	–
1Δ	hulsite	Δ	$(Fe,Mg)_2(Fe,Sn)O_2[BO_3]$	10.695(4)	3.102(1)	5.431(1)	–	94.21(3)	–	*P2/m*	(17)	–
1Δ	magnesiohulsite	Δ	$(Mg,Fe)_2(Fe,Sn)O_2[BO_3]$	–	–	–	–	–	–	–	(18)	–
1Δ	jimboite	Δ	$Mn_3[BO_3]_2$	5.658(1)	8.740(1)	4.646(2)	–	–	–	*Pnmn*	(21)	–
1Δ	kotoite	Δ	$Mg_3[BO_3]_2$	5.396(1)	8.297(2)	4.459(1)	–	–	–	*Pnmn*	(22)	3a
1Δ	nordenskiöldine	Δ	$CaSn[BO_3]_2$	4.858(1)	4.858(1)	16.080(2)	–	–	–	$R\bar{3}$	(23)	–
1Δ	tusionite	Δ	$MnSn[BO_3]_2$	4.781(1)	4.781(1)	15.381(7)	–	–	–	$R\bar{3}$	(24)	–
1□	sinhalite	□	$AlMg[BO_4]$	9.878	5.675	4.328	–	–	–	*Pnma*	(26)	–
1Δ	sassolite	Δ	$[B(OH)_3]$	7.039	7.053	6.578	92.58	101.17	119.83	$P\bar{1}$	(25)	3b
1□	bandylite	□	$Cu[B(OH)_4]Cl$	6.19	6.19	5.61	–	–	–	*P4/n*	(27)	4a
1□	teepleite	□	$Na_2[B(OH)_4]Cl$	7.260(2)	7.260(2)	4.847(2)	–	–	–	*P4/nnm*	(28)	4b
1□	frolovite	□	$Ca[B(OH)_4]_2$	7.774(2)	5.680(1)	8.136(2)	11.315(1)	101.67(2)	107.87(2)	$P\bar{1}$	(29)	4c
1□	hexahydroborite	□	$Ca[B(OH)_4]_2(H_2O)_2$	8.006(2)	8.012(2)	6.649(2)	–	–	104.21(2)	*P2/a*	(30)	4d
1□	henmilite	□	$Ca_2Cu(OH)_4[B(OH)_4]_2$	5.7617(5)	7.9774(6)	5.6488(4)	109.611(6)	91.473(7)	83.686(7)	$P\bar{1}$	(31)	4e

* Group named after this mineral; ** formulae given by Cooper & Hawthorne (1998).

(1) Konev *et al.* (1970), (2) De Waal *et al.* (1974), (3) Burns *et al.* (1994), (4) Bonazzi & Menchetti (1989), (5) Swinnea & Steinfink (1983), (6) Alfredsson *et al.* (1991), (7) Takéuchi *et al.* (1978), (8) Norrestam & Bovin (1987), (9) Cooper & Hawthorne (1998) (10) Bovin *et al.* (1996), (11) Moore & Araki (1974a), (12) Dal Negro & Tadini (1974), (13) Moore & Araki (1976), (14) Sokolova *et al.* (1987), (15) Bigi *et al.* (1991), (16) Huang & Wang (1994), (17) Yamanova *et al.* (1978), (18) Yang *et al.* (1985), (19) Bonazzi *et al.* (1986), (20) Moore & Araki (1972a), (21) Bondareva *et al.* (1978), (22) Effenberger & Pertlik (1984), (23) Effenberger & Zemann (1986), (24) Cooper *et al.* (1994), (25) Zachariasen (1954), (26) Fang & Newnham (1965), (27) Collin (1951), (28) Effenberger (1982), (29) Simonov *et al.* (1976a), (30) Simonov *et al.* (1976b), (31) Nakai *et al.* (1986)

the stoichiometries of such structures, it is important to remember that the terminal octahedra of the *F* wall and the *C* wall are common to each unit, and should not be counted twice.) For ludwigite, $n = 3$, for orthopinakiolite, $n = 5$, for takéuchiite, $n = 7$, and for blatterite, $n = 9$. The next (unnamed) member of this series has $n = 11$; details of the unit cell are given in Table 1. Pinakiolite (Fig. 1) is the end-member of this series: $F_\infty C_\infty S_\infty$.

In all of these structures, the direction of the wall is changed [in the (001) plane] by a glide operation orthogonal to [100]. If $c \approx 3$ Å (as in ludwigite), this operation is a *b* glide; if $c \approx 6$ Å (as in orthopinakiolite, takéuchiite and blatterite, Table 1), this operation is an *n* glide. The type of glide plane is related to the chemical composition and stereochemistry of the *F* wall. The ludwigite minerals have chemically and structurally simple *F*-walls that are compatible with a *c*-repeat of only 3 Å (*i.e.*, one octahedron along the *c* axis). The other zigzag borates have chemically (and structurally) more complicated *F*-walls, and hence require a longer repeat-distance in the *c* direction to incorporate these

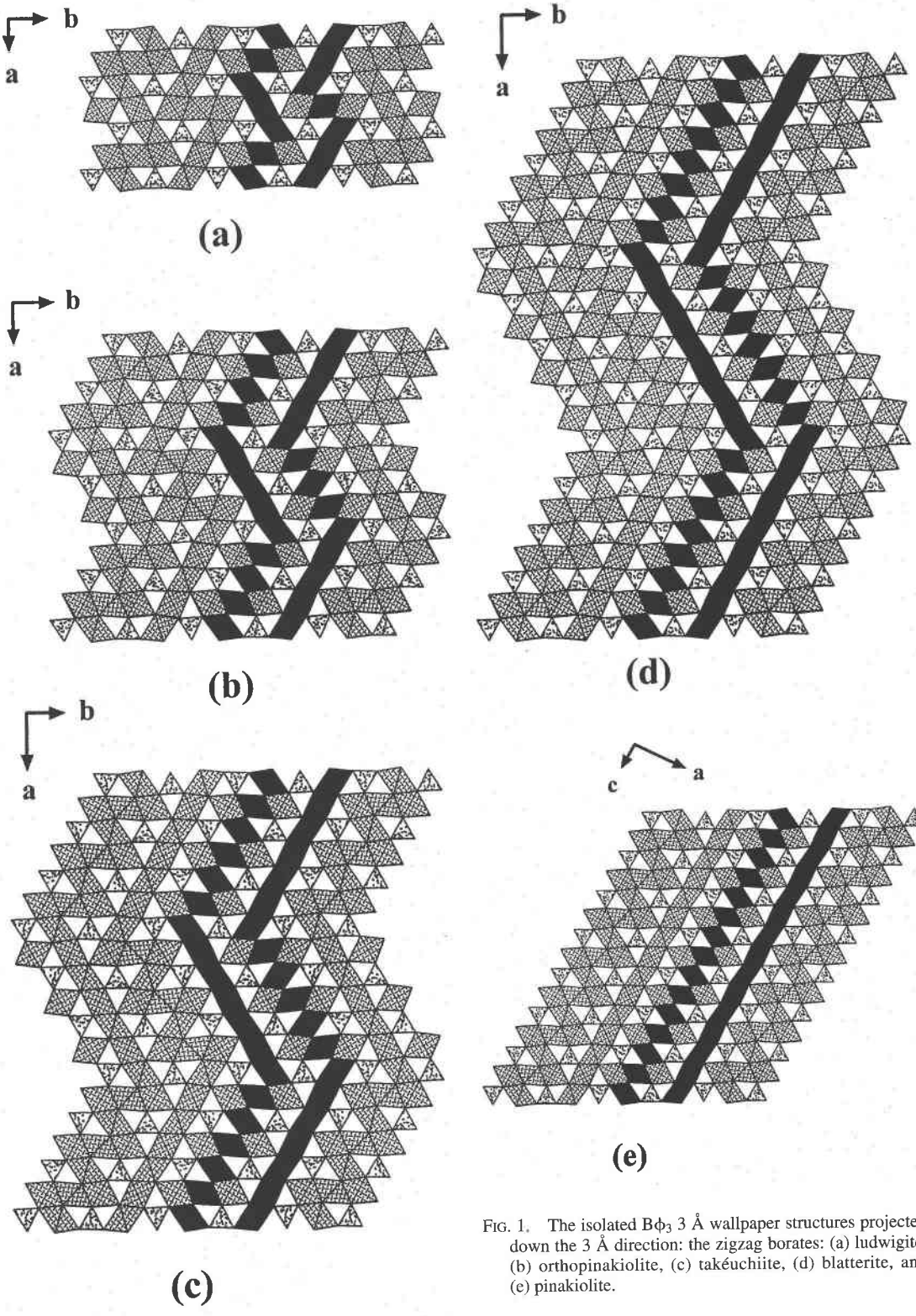

FIG. 1. The isolated $B\phi_3$ 3 Å wallpaper structures projected down the 3 Å direction: the zigzag borates: (a) ludwigite, (b) orthopinakiolite, (c) takéuchiite, (d) blatterite, and (e) pinakiolite.

more complicated chemical compositions. An *n* glide gives double the repeat distance in the *c* direction for the *F* wall which, when combined with the increase in the *a* dimension, gives sufficient room for the *F* wall to incorporate the required combination of different types of cation sites.

The *C* wall in these minerals shows extreme positional disorder of its constituent cations, the degree of which increases with increasing *n* in the formula $F_nC_nS_n$. This makes determination of the correct chemical formula quite difficult. However, it is clear from the structural results that the general formula $M^{2+}{}_2(M^{3+},M^{5+})(BO_3)O_2$ is inappropriate. These structures are not all polymorphs. Indeed, the occurrence of blatterite seems to be due to the need to incorporate Sb^{5+} into the *F* wall, and a complicated formula results (Table 1). It is feasible that the structural differences in these $F_nC_nS_n$ structures are driven by slight compositional differences. Certainly, the occurrence of all these structure types at a single locality poses some interesting questions on paragenesis.

Other wallpaper structures: The simplest structure is that of fluoborite, $[Mg_3(BO_3)(F,OH)_2]$, in which chains of octahedra occur in pairs that share vertices to form a triangular tunnel, which contains the ($B\phi_3$) groups (Fig. 2a); the hexagonal tunnels are empty in fluoborite. Painite, $CaZr[BAl_9O_{18}]$, has the same structure in projection despite the very different chemical composition. The octahedra in painite are occupied by Al, reducing the basic repeat-length of the chain from 3.0 to 2.8 Å. In addition, only alternate triangular tunnels are occupied by ($B\phi_3$) groups; the other triangular tunnels contain Zr in trigonal prismatic coordination, leading to a tripling of the repeat distance along the chain-repeat direction. The hexagonal tunnels, empty in fluoborite, are occupied by [6]-coordinated Ca in painite. Jeremejevite, $[Al_6(BO_3)_5(OH)_3]$, also has a similar framework to that of fluoborite, except that every third octahedral site along the chain-repeat direction is vacant, and the resulting octahedral dimers are linked along the chain direction by BO_3 triangles.

In warwickite, $[(Mg,Ti)_2(BO_3)O]$, the chains of octahedra share edges to form ribbons four octahedra wide; each ribbon is canted at 60° to the adjacent ribbons, and the resulting triangular interstices are bridged by BO_3 triangles (Fig. 2b). Karlite, $Mg_7(OH)_4(BO_3)_4Cl$, consists of 2 × 1 edge-sharing ribbons of $[M\phi_4]$ chains (Fig. 2c) and simple (1 × 1) $[M\phi_4]$ chains linked in the 3^6 plane by sharing octahedron vertices to form large octagonal channels parallel to [001]. The sequence of octahedra around each channel is 2–1–1–2–1–1 (Fig. 2c), and the large Cl anion occurs in these channels. Wightmanite, $[Mg_5(BO_3)(OH)_5O](H_2O)_2$, consists of 2 × 2 edge-sharing bundles of $[M\phi_4]$ chains and 1 × 2 ribbons of edge-sharing chains (Fig. 2d), linked in the 3^6 plane by sharing vertices of octahedra and by (BO_3) groups in the resulting triangular channels through the framework. Large hexagonal channels through the structure are filled with disordered (H_2O) groups.

FBB = 1Δ:Δ, φ = O^{2-}; miscellaneous structures

The minerals of the kotoite group are based on a $[M_3(B\phi_3)_2]$ framework of corner-sharing between triangles and octahedra, and edge-sharing between octahedra (Fig. 3a). Two octahedra share edges to form a dimer, and these dimers alternate with single octahedra along [100] to form a chain of edge-sharing octahedra of the form $[M_3\phi_{10}]$. These chains cross-link along [010] by sharing corners with isolated $B\phi_3$ triangles to form sheets parallel to (001) that link into a framework by sharing corners with linking triangles and octahedra.

Nordenskioldine and tusionite are isostructural with dolomite, with Ca and Mn proxying for Ca, and Sn^{4+} proxying for Mg in the prototype dolomite structure.

FBB = 1Δ:Δ, φ = OH^-

Sassolite, $[B(OH)_3]$, is the only mineral in this subgroup. The structure (Fig. 3b) consists of layers of $B(OH)_3$ triangles H-bonded together to form a sheet parallel to (001). Adjacent sheets are separated by 3.16 Å, and the intersheet attraction is assured by weak Van der Waals interactions.

FBB = 1□:□, φ = O^{2-}

There is only one mineral within this class, sinhalite, $AlMg(BO_4)$. Sinhalite is isostructural with olivine, with Al occupying the *M*1 site and Mg occupying the *M*2 site. It is a compact close-packed structure.

FBB = 1□:□, φ = OH^-

In bandylite, $Cu[B(OH)_4]Cl$, there is one unique Cu^{2+} atom that is octahedrally coordinated by four (OH) groups and two Cl atoms; ($Cu^{2+}\phi_6$) octahedra and ($B\phi_4$) tetrahedra link by sharing corners to form a distorted chequerboard of corner-sharing polyhedra (Fig. 4a) parallel to (001). The ($Cu^{2+}\phi_6$) octahedra show the usual Jahn–Teller distortion, with Cl as the apical ligand at a distance of 2.8 Å. Sheets adjacent along [001] link through apical Cl atoms of the ($Cu\phi_6$) polyhedra, forming $[Cu\phi_5]$ chains of corner-sharing octahedra parallel to the *c* axis. In teeplite, $Na_2[B(OH)_4]Cl$, there is one unique Na atom coordinated by four (OH) groups and two Cl atoms. ($Na\phi_6$) octahedra are cross-linked by edge-sharing into a sheet orthogonal to [001]. These sheets stack along the *c* axis, and adjacent sheets are linked by ($Na\phi_6$)–($B\phi_4$) corner-sharing with layers of ($B\phi_4$) tetrahedra in the (001) plane (Fig. 4b). The ($Na\phi_6$) octahedra have four meridional OH ligands and two apical Cl ligands, and the octahedra are canted such that each Cl atom is coordinated by four Na atoms.

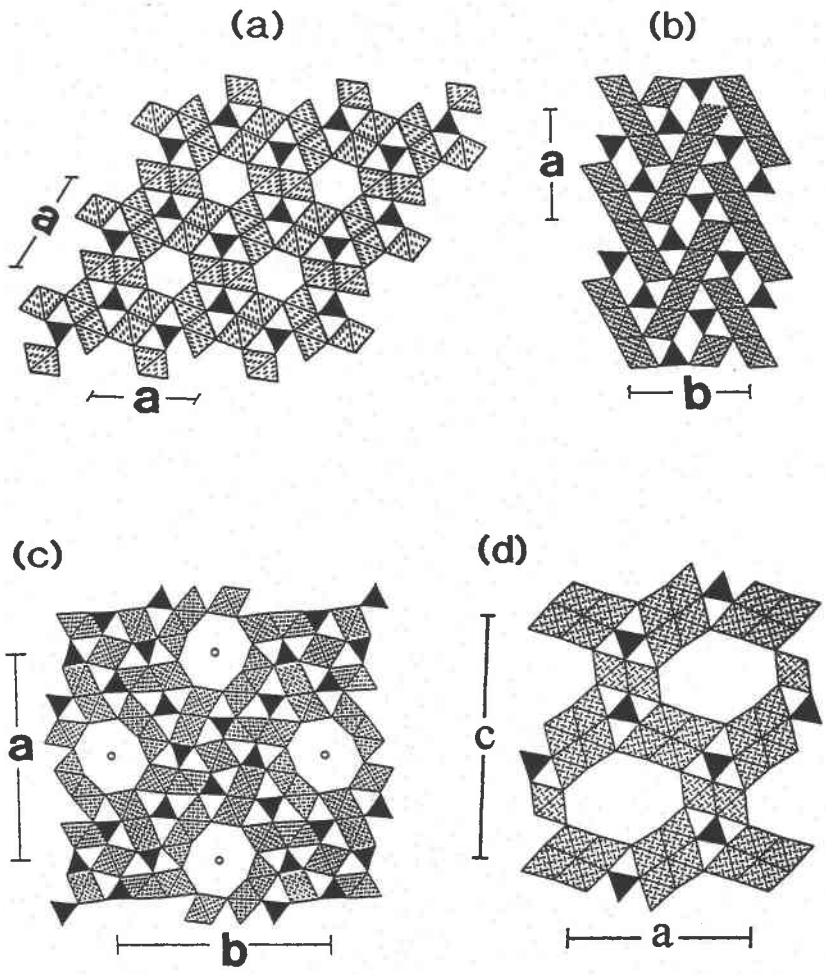

FIG. 2. The isolated $B\phi_3$ 3 Å wallpaper structures projected down the 3 Å direction: miscellaneous structures: (a) fluoborite, (b) warwickite, (c) karlite, and (d) wightmanite. Divalent- and trivalent-occupant octahedra are random-dot shaded, BO_3 triangles are shown in black.

Frolovite, $Ca\{B(OH)_4\}_2$, has one unique Ca atom that is coordinated by eight (OH) groups. The ($Ca\phi_8$) polyhedra share edges to form $[Ca_2\phi_{14}]$ dimers that are cross-linked by $\{B(OH)_4\}$ tetrahedra to form $[Ca\{B(OH)_4\}_2]$ sheets parallel to {101}; an oblique view of this sheet is shown in Figure 4c. These sheets are neutral, and are linked solely by H-bonding, accounting for the prominent {101} cleavage of frolovite. Hexahydroborite, $Ca[B(OH)_4]_2(H_2O)_2$, consists of chains of edge-sharing ($Ca\phi_8$) polyhedra extending along [100] and decorated by $\{B(OH)_4\}$ tetrahedra (Fig. 4d). The chains are linked in the other two dimensions by H bonding that involves an interstitial (H_2O) group that is not bonded to any cation. In henmilite, $Ca_2Cu(OH)_4(B(OH)_4)_2$, there is one unique Ca atom coordinated by eight (OH) groups. Pairs of ($Ca\phi_8$) polyhedra share edges to form $[Ca_2\phi_{14}]$ dimers that are linked into chains along [001] by $\{B(OH)_4\}$ tetrahedra. These chains are cross-linked by square-planar ($Cu\phi_4$) groups (Fig. 4e) into a three-dimensional network that is strengthened by H-bonding.

STRUCTURES BASED ON FINITE CLUSTERS OF POLYHEDRA

At present, there are twelve distinct types of clusters known, and these may be divided into seven sets: (1) 2B:2B, (2) 3B:<3B>, (3) 4B:<3B>B, (4) 5B:<3B>–<3B>, (5) 4B:<3B>=<3B>, (6) 6B:[ϕ]<3B> | <3B> | <3B> |, and (7) 15B:{<3B>–<3B>}. The minerals in

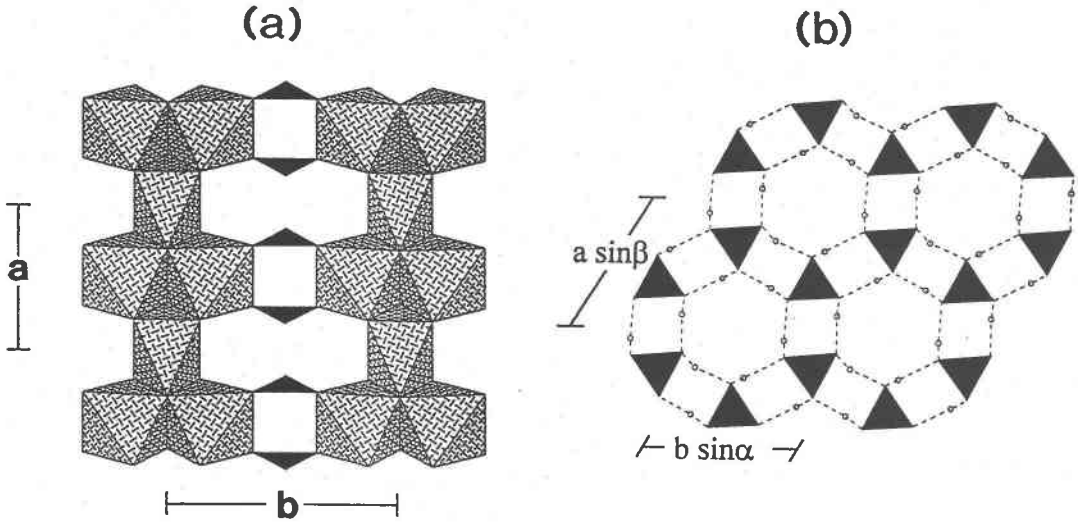

FIG. 3. Miscellaneous isolated $B\phi_3$ polyhedra structures: (a) kotoite, and (b) sassolite.

TABLE 2. BORATE MINERALS BASED ON FINITE CLUSTERS OF $B\Phi_3$ AND $B\Phi_4$ POLYHEDRA

Polyhedra	Name	Connectivity	Formula	*a* (Å)	*b* (Å)	*c* (Å)	β (°)	Sp.Gr.	Ref. Fig.
			3Å wallpaper structures						
2Δ	suanite	2Δ	$Mg_2[B_2O_5]$	12.10(5)	3.12(2)	9.36(5)	104.3(5)	$P2_1/a$	(1) 6a
2Δ	száibélyite	2Δ	$Mg_2(OH)[B_2O_4(OH)]$	3.139(1)	10.393(2)	12.577(2)	95.88(2)	$P2_1/c$	(2) 6b
2Δ	sussexite	2Δ	$Mn_2(OH)[B_2O_4(OH)]$	3.287(1)	10.718(2)	12.866(3)	94.75(3)	$P2_1/c$	(2) –
2Δ	kurchatovite	2Δ	$CaMg[B_2O_5]$	12.331(4)	5.489(1)	11.092(4)	–	$P2_1/b$	(3) 6c
2□	pentahydroborite	2□	$Ca[B_2O(OH)_8](H_2O)_2$	7.875(2)	6.534(2)	8.104(2)	111.33	$P\bar{1}$	(4) 6d
2□	pinnoite	2□	$Mg[B_2O(OH)_6]$	7.614(1)	7.614(1)	8.1898(8)	–	$P4_2$	(5) 6e
2Δ1□	ameghinite	⟨2Δ□⟩	$Na[B_3O_3(OH)_4]$	18.428(3)	9.882(2)	6.326(2)	104.38(1)	$C2/c$	(6) 6f
1Δ2□	inderite	⟨Δ2□⟩	$Mg[B_3O_3(OH)_5](H_2O)_5$	6.8221(3)	13.1145(13)	12.0350(8)	104.552(8)	$P2_1/c$	(7) 7a
1Δ2□	kurnakovite	⟨Δ2□⟩	$Mg[B_3O_3(OH)_5](H_2O)_5$	8.3479	10.6068	6.4447	108.891	$P\bar{1}$	(8) 7b
1Δ2□	inyoite	⟨Δ2□⟩	$Ca[B_3O_3(OH)_5](H_2O)_4$	10.63	12.06	8.405	114.03(8)	$P2_1/a$	(9) 7c
1Δ2□	meyerhofferite	⟨Δ2□⟩	$Ca[B_3O_3(OH)_5](H_2O)$	6.632(1)	8.337(1)	6.4748(6)	101.97(1)	$P\bar{1}$	(10) 7d
1Δ2□	solongoite	⟨Δ2□⟩	$Ca_2[B_3O_4(OH)_4]Cl$	7.955(3)	12.570(5)	7.241(3)	–	$P2_1/b$	(11) 7e
1Δ2□	inderborite	⟨Δ2□⟩	$CaMg[B_3O_3(OH)_5]_2(H_2O)_5$	12.137(2)	7.433(1)	19.234(3)	90.29(1)	$C2/c$	(12) 7f
3□	nifontovite	⟨3□⟩	$Ca_3[B_3O_3(OH)_6]_2(H_2O)_2$	13.119(4)	13.445(5)	9.526(3)	–	$B2/b$	(13) 8a
2Δ2□	hydrochlorborite	⟨Δ2□⟩Δ	$Ca_2[B_3O_3(OH)_4][BO(OH)_3]Cl(H_2O)_7$	22.783(3)	8.745(1)	17.066(1)	96.705(1)	$I2/a$	(14) 8b
4□	uralborite	⟨3□⟩□	$Ca_2[B_4O_4(OH)_8]$	6.927(3)	9.836(3)	12.331(3)	–	$P2_1/n$	(15) 8c
4Δ1□	sborgite	⟨2Δ□⟩-⟨2Δ□⟩	$Na[B_4O_6(OH)_4](H_2O)_3$	11.119	16.474	13.576	112.83	$C2/c$	(16) 8d
2Δ3□	ulexite	⟨Δ2□⟩-⟨Δ2□⟩	$NaCa[B_5O_6(OH)_6](H_2O)_5$	8.816(3)	12.870(7)	6.678(1)	109.05(2)	$P\bar{1}$	(17) 8e
2Δ2□	borax	⟨Δ2□⟩=⟨Δ2□⟩	$Na_2[B_4O_5(OH)_4](H_2O)_8$	11.885(1)	10.654(1)	12.206(1)	106.623(5)	$C2/c$	(18) 9a
2Δ2□	tincalconite	⟨Δ2□⟩=⟨Δ2□⟩	$Na_2[B_4O_5(OH)_4](H_2O)_3$	11.097(2)	11.097(2)	21.114(4)	–	$R32$	(19) 9b
2Δ2□	hungchaoite	⟨Δ2□⟩=⟨Δ2□⟩	$Mg[B_4O_5(OH)_4](H_2O)_7$	8.807(1)	10.657(1)	7.897(1)	108.53(1)	$P\bar{1}$	(20) 9c
2Δ2□	fedorovskite	⟨Δ2□⟩=⟨Δ2□⟩	$Ca_2Mg_2(OH)_4[B_4O_7(OH)_2]$	8.96(2)	13.15(2)	8.15(1)	–	$Pbam$	(21) –
2Δ2□	roweite	⟨Δ2□⟩=⟨Δ2□⟩	$Ca_2Mn_2(OH)_4[B_4O_7(OH)_2]$	9.057(1)	13.357(2)	8.289(1)	–	$Pbam$	(22) 9d
3Δ3□	mcallisterite	[ϕ]⟨Δ2□⟩|⟨Δ2□⟩|⟨Δ2□⟩|	$Mg_2[B_6O_7(OH)_6]_2(H_2O)_9$	11.549(2)	11.549(2)	35.567(8)	–	$R\bar{3}c$	(23) 10a
3Δ3□	aksaite	[ϕ]⟨Δ2□⟩|⟨Δ2□⟩|⟨Δ2□⟩|	$Mg[B_6O_7(OH)_6](H_2O)_2$	12.540(6)	24.327(11)	7.480(3)	–	$Pbca$	(24) 10b
3Δ3□	rivadavite	[ϕ]⟨Δ2□⟩|⟨Δ2□⟩|⟨Δ2□⟩|	$Na_4Mg[B_6O_7(OH)_6]_4(H_2O)_{10}$	15.870	8.010	22.256	116.43	$P2_1/c$	(25) –
12Δ3□	ammonioborite	3(⟨2Δ□⟩-⟨2Δ□⟩)	$(NH_4)_3[B_{15}O_{20}(OH)_8](H_2O)_4$	25.27	9.65	11.56	94.28	$C2/c$	(26) 10c

kurchatovite: γ=78.7(2)°; pentahydroborite: α=111.53°, γ=72.70°; kurnakovite: α=98.846°, γ=105.581°; meyerhofferite: α=90.81(1)°, γ=86.76(1)°; solongoite: α=86.18(5)°; nifontovite: γ=118.40(2)°; uralborite: γ=97.81(3)°; ulexite: α=90.36(2)°, γ=104.98(4)°; hungchaoite: α=103.39(1)°, γ=97.18(1)°

(1) Takéuchi (1952), (2) Takéuchi & Kudoh (1975), Hoffman & Armbruster (1995), (3) Yakubovich *et al.* (1976), (4) Kazanskaya *et al.* (1977), (5) Genkina & Malinovskii (1983), (6) Dal Negro *et al.* (1975), (7) Corazza (1976), (8) Corazza (1974), (9) Clark *et al.* (1964), (10) Burns & Hawthorne (1993b), (11) Yamanova *et al.* (1977) (12) Burns & Hawthorne (1994c), (13) Simonov *et al.* (1978), (14) Brown & Clark (1978), (15) Simonov *et al.* (1977), (16) Merlino & Sartori (1972), (17) Ghose & Clark (1978), (18) Levy & Lisensky (1978), (19) Powell *et al.* (1991), (20) Wan & Ghose (1977), (21) Malinko *et al.* (1976), (22) Moore & Araki (1974b), (23) Dal Negro *et al.* (1969), (24) Dal Negro *et al.* (1971), (25) Dal Negro *et al.* (1973), (26) Merlino & Sartori (1971)

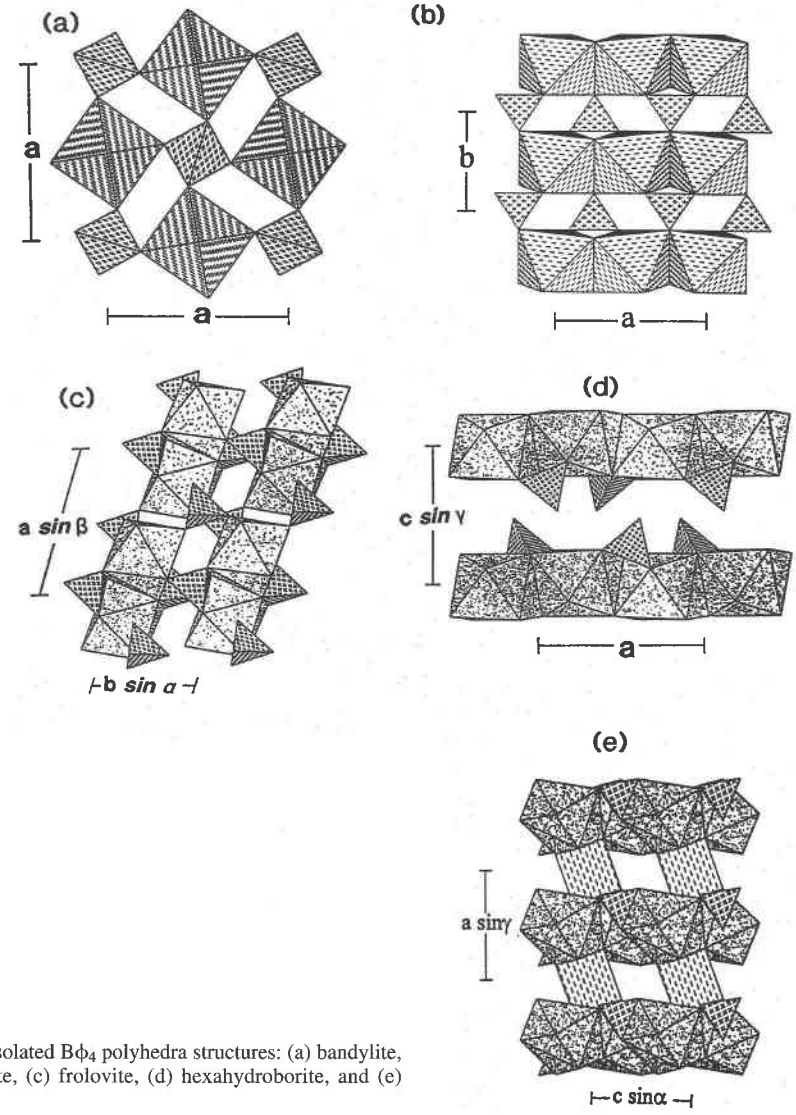

FIG. 4. The isolated $B\phi_4$ polyhedra structures: (a) bandylite, (b) teepleite, (c) frolovite, (d) hexahydroborite, and (e) henmilite.

this class are listed in Table 2; the clusters are illustrated in Figure 5.

FBB = 2Δ:2Δ

This *FBB* (Fig. 5a) occurs as an isolated cluster in four minerals. Two minerals of this set have wallpaper structures and show very strong affinities with the *FBB* = 1Δ:Δ wallpaper structures (Figs. 1, 2). Suanite consists of ribbons of parallel edge-sharing octahedra, four octahedra wide, that extend in the [010] direction and are cross-linked in the (101) plane by $[B_2O_5]$ groups (Fig. 6a). Száibélyite and sussexite are isostructural, and consist of 1 × 2 ribbons of edge-sharing octahedra that link by sharing vertices to form corrugated sheets of octahedra perpendicular to [100] (Fig. 6b); these sheets are cross-linked into a framework by $[B_2O_5]$ groups.

In kurchatovite, $CaMgB_2O_5$, (MgO_6) octahedra share corners to form a chequerboard pattern resembling a slice through the perovskite structure. These $[MgO_4]$ sheets are linked along [001] by $[B_2O_5]$ groups. One (BO_3) group links to two apical vertices of octahedra from adjacent sheets, and the other (BO_3) group links to two meridional vertices of octahedra from the same sheet (Fig. 6c). Seven-coordinated Ca further links the $[MgO_4]$ sheets to form a fairly dense-packed structure.

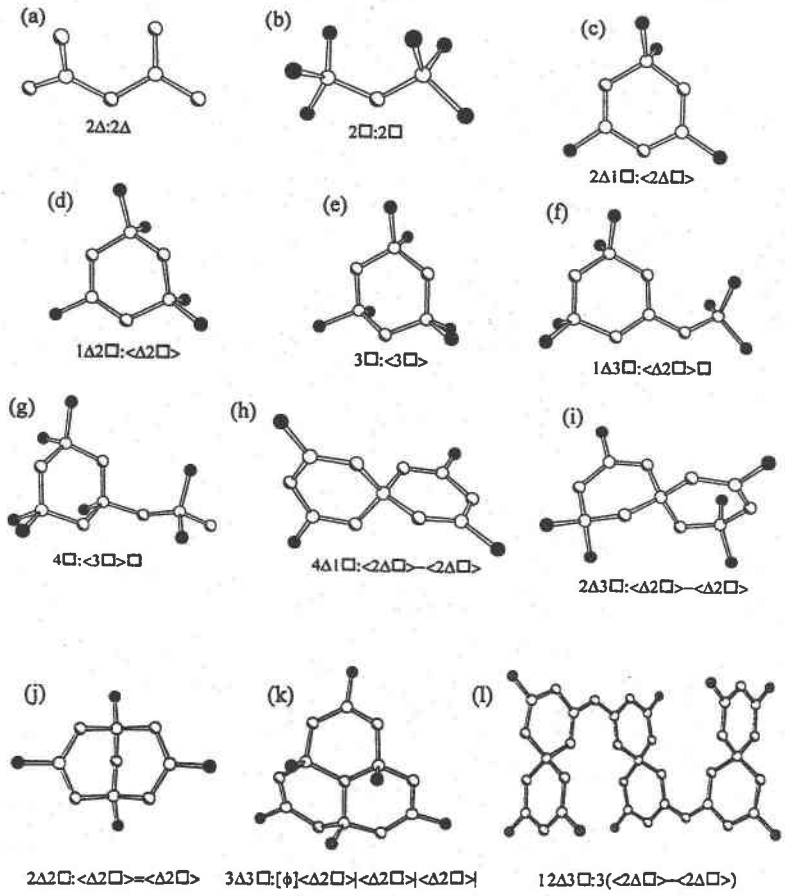

FIG. 5. The twelve distinct clusters that occur as *FBB*s in the finite-cluster borate minerals.

FBB = 2□:2□

Two minerals contain this *FBB* (Fig. 5b) as an isolated cluster in their structure. In both cases, two ($B\phi_4$) groups share a vertex to form a $[B_2O(OH)_6]$ cluster. In pentahydroborite, $Ca[B_2O(OH)_6](H_2O)_2$, there is one unique Ca atom coordinated by one O atom, three (OH) groups and one (H_2O) group. The ($Ca\phi_7$) polyhedra share edges to form $[Ca_2\phi_{12}]$ dimers that are cross-linked by $[B_2\phi_7]$ groups to form corrugated sheets parallel to (100) (Fig. 6d). These sheets are linked directly *via* H-bonds involving the (OH) anions of the pyroborate group and the (H_2O) groups that bond directly to the Ca atoms. In pinnoite, $Mg[B_2O(OH)_6]$, there is one unique Mg atom octahedrally coordinated by O atoms and (OH) groups. The ($Mg\phi_6$) octahedra and $[B_2\phi_7]$ pyroborate groups cross-link into a framework. Each (OH) ligand of the borate group links directly to one ($Mg\phi_6$) octahedron (Fig. 6e), and H-bonds to the bridging O anion of adjacent pyroborate groups.

FBB = 2Δ1□:<2Δ□>

This *FBB* occurs in ameghinite, $Na[B_3O_3(OH)_4]$, as an isolated <2Δ□> cluster of the form $[B_3O_3(OH)_4]$ (Fig. 5c). There is one unique Na atom octahedrally coordinated by one O atom and five (OH) groups, and each pair of ($Na\phi_6$) octahedra share an edge to form $[Na\phi_{10}]$ dimers. Each ($Na\phi_6$) octahedron links to five <2Δ□> clusters to form a framework (Fig. 6f). This framework has a distinctly layered aspect, with sheets at $y \approx \pm 1/4$, and extensive H-bonding provides further inter-cluster linkage.

FBB = 1Δ2□:<Δ2□>

There are six finite-cluster structures with this *FBB* (Fig. 5d), which also occurs polymerized into chains (see below). Inderite and kurnakovite are polymorphs of composition $Mg[B_3O_3(OH)_5](H_2O)_5$. In inderite (Fig. 7a), there is one unique Mg site that is coordinated

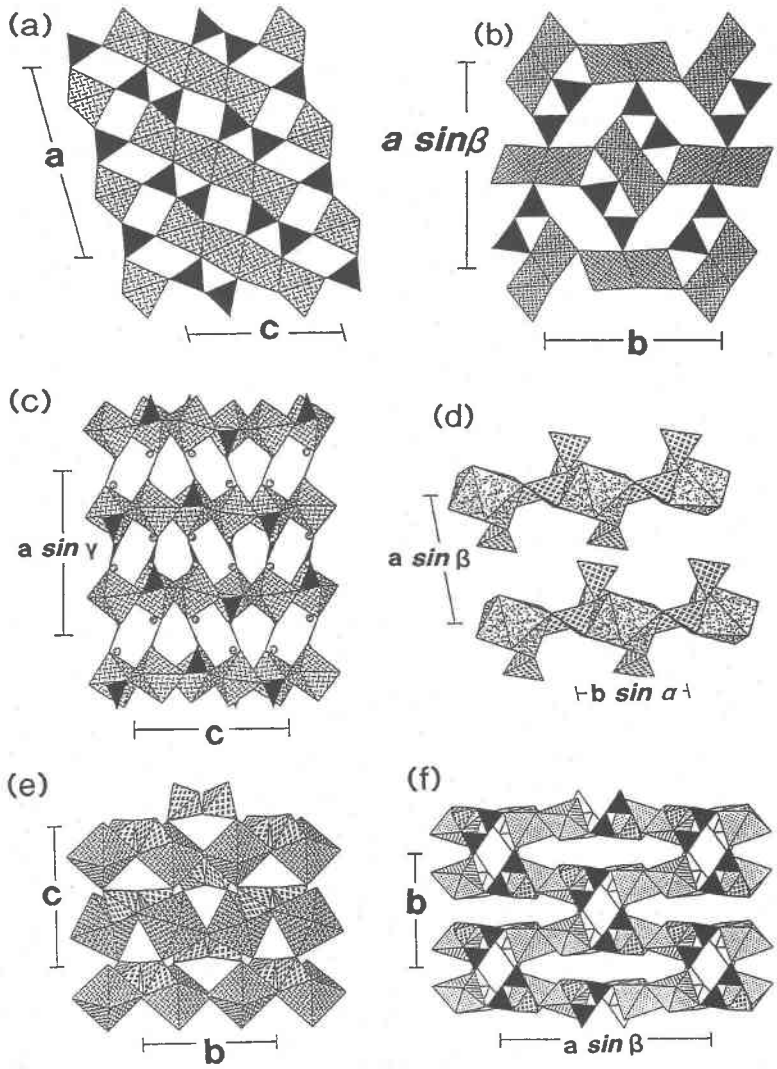

FIG. 6. Finite-cluster borate structures containing the *FBBs* 2Δ:2Δ, 2□2□ and 2Δ1□:<2Δ□>: (a) suanite, (b) szaibélyite, (c) kurchatovite, (d) pentahydroborite, (e) pinnoite, and (f) ameghinite.

by two (OH) groups and four (H_2O) groups. Each <Δ2□> ring links to one ($Mg\phi_6$) octahedron by sharing two vertices of different (BO_4) groups with an edge of the octahedron; the result is a cluster of composition $Mg[B_3O_3(OH)_5](H_2O)_4$. These clusters are linked only by H-bonding, both directly *via* the (OH) and (H_2O) ligands of the cluster, and through the single interstitial (H_2O) group. In kurnakovite, there is one unique Mg site octahedrally coordinated by two (OH) groups and four (H_2O) groups. Each <Δ2□> ring links to two (symmetrically equivalent) ($Mg\phi_6$) octahedra to form chains that extend parallel to [001] (Fig. 7b); the chain in kurnakovite has the same stoichiometry as the cluster in inderite. Interchain linkage is *via* direct H-bonding and also *via* H-bonding involving the single interstitial (H_2O) group.

In inyoite, $Ca[B_3O_3(OH)_5](H_2O)_4$, there is one unique Ca atom coordinated by two O atoms, three (OH) groups and three (H_2O) groups. Two ($Ca\phi_8$) polyhedra share an edge to form a dimer of composition $[Ca_2\phi_{14}]$. Each <Δ2□> cluster shares two tetrahedron edges with one ($Ca\phi_8$) polyhedron and one tetrahedron vertex with

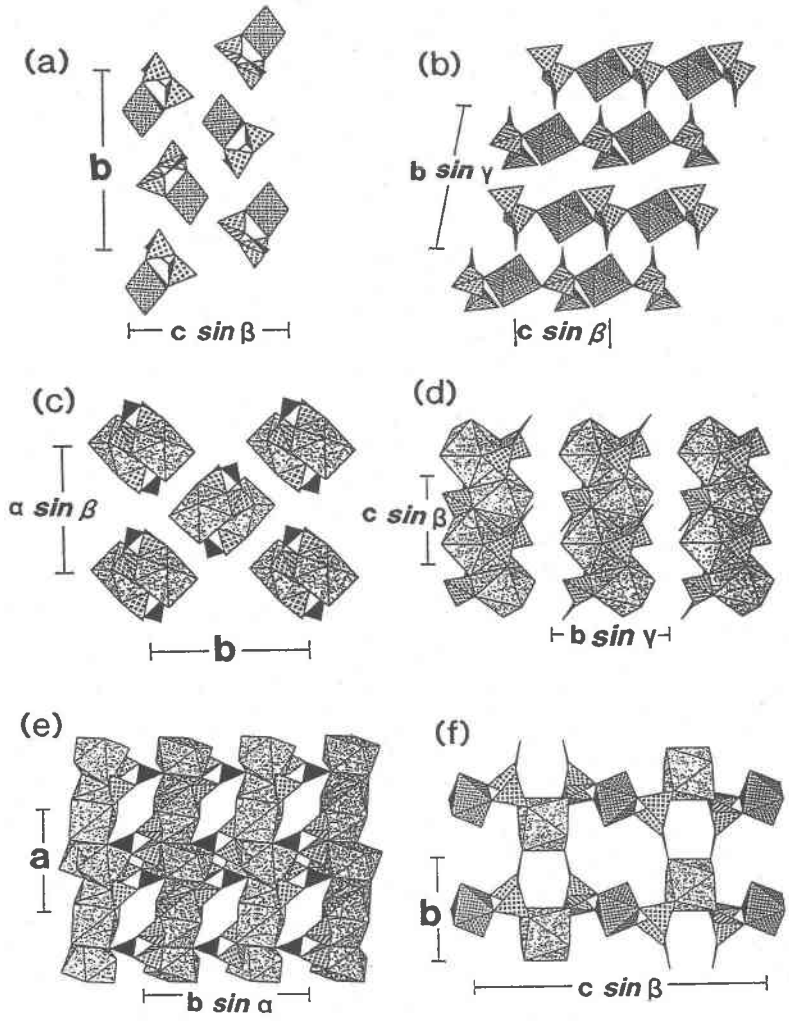

FIG. 7. Finite-cluster borate structures containing the *FBB* 1Δ2:<Δ2□>: (a) inderite, (b) kurnakovite, (c) inyoite, (d) meyerhofferite, (e) solongoite, and (f) inderborite.

the other ($Ca\phi_8$) polyhedron of the dimer (Fig. 7c). These clusters are joined solely by H-bonding. In meyerhofferite, $Ca[B_3O_3(OH)_5](H_2O)$, there is one unique Ca atom coordinated by three O atoms, four (OH) groups and one (H_2O) group, and ($Ca\phi_8$) polyhedra share edges to form zigzag chains parallel to [001] (Fig. 7d). Each <Δ2□> ring attaches to three ($Ca\phi_8$) polyhedra, each of which is adjacent in the same chain. Each (BO_4) tetrahedron shares edges with two different ($Ca\phi_8$) polyhedra, and the (BO_3) triangle attaches to a ($Ca\phi_8$) polyhedron by corner-sharing (Fig. 7d). There are no interstitial (H_2O) groups, and interchain linkage involves H-bonding directly between the chains.

In solongoite, $Ca_2[B_3O_4(OH)_4]Cl$, there are two unique Ca atoms; one Ca is coordinated by two O atoms, four (OH) groups and two Cl atoms, and the other Ca is coordinated by four O atoms and four (OH) groups. The ($Ca\phi_8$) groups polymerize to form sheets of edge-sharing ($Ca\phi_8$) polyhedra parallel to (010) (Fig. 7e) that are cross-linked by <Δ2□> rings. Both (BO_4) tetrahedra share edges with the ($Ca\phi_8$) polyhedra, and the (BO_3) triangle extends outward from the sheet to link by corner-sharing to the adjacent sheet. Inderborite, $CaMg[B_3O_3(OH)_5]_2(H_2O)_6$, is the most complex structure of this particular group. The borate tetrahedra of two <Δ2□> rings each share a corner with

the ($Mg\phi_6$) octahedron (Fig. 7f); one tetrahedron shares a non-bridging anion, and both tetrahedra share a bridging anion with a single ($Ca\phi_8$) polyhedron, forming infinite rods parallel to [001] that cross-link *via* corner-sharing between (BO_3) and ($Ca\phi_8$) groups (Fig. 7f). These sheets are then cross-linked by H-bonding both directly between the sheets and *via* interstitial (H_2O) groups.

FBB = *3□:<3□>*

This *FBB* (Fig. 5e) occurs as isolated clusters in nifontovite, $Ca_3[B_3O_3(OH)_6](H_2O)_2$, and it also polymerizes to form a framework structure in metaborite (see below). In nifontovite, there are two distinct Ca atoms, each of which is [8]-coordinated by O atoms, (OH) groups and (H_2O) groups. The ($Ca\phi_8$) polyhedra share edges to form chains extending along [101]. These chains are cross-linked by <3□> rings, which share both edges and corners with ($Ca\phi_8$) polyhedra (Fig. 8a), together with a network of H-bonds.

FBB = *1Δ3□:<Δ2□>□*

This *FBB* occurs only in hydrochlorborite, $Ca_2[B_3O_3(OH)_4][BO(OH)_3]Cl(H_2O)_7$, the only example of a cluster mineral with a decorated <Δ2□> ring (Fig. 5f). There are two unique Ca atoms, each coordinated by two O atoms, three (OH) groups and three (H_2O) groups. The ($Ca\phi_8$) polyhedra link to form a four-membered linear cluster, two central polyhedra sharing an edge and the two outer polyhedra linking to the central edge-sharing dimer by corner-sharing. Each ($Ca\phi_8$) polyhedron shares two edges with borate tetrahedra of the <Δ2□> ring, and the (BO_3) triangle bridges to an adjacent ($Ca\phi_8$) polyhedron (Fig. 8b). The resulting structural unit consists of heteropolyhedral chains extending along *a*. Cross-linkage of these chains occurs *via* H-bonding, both directly from one chain to another, and also *via* an interstitial (H_2O) group and a Cl anion that is an acceptor for eight H-bonds.

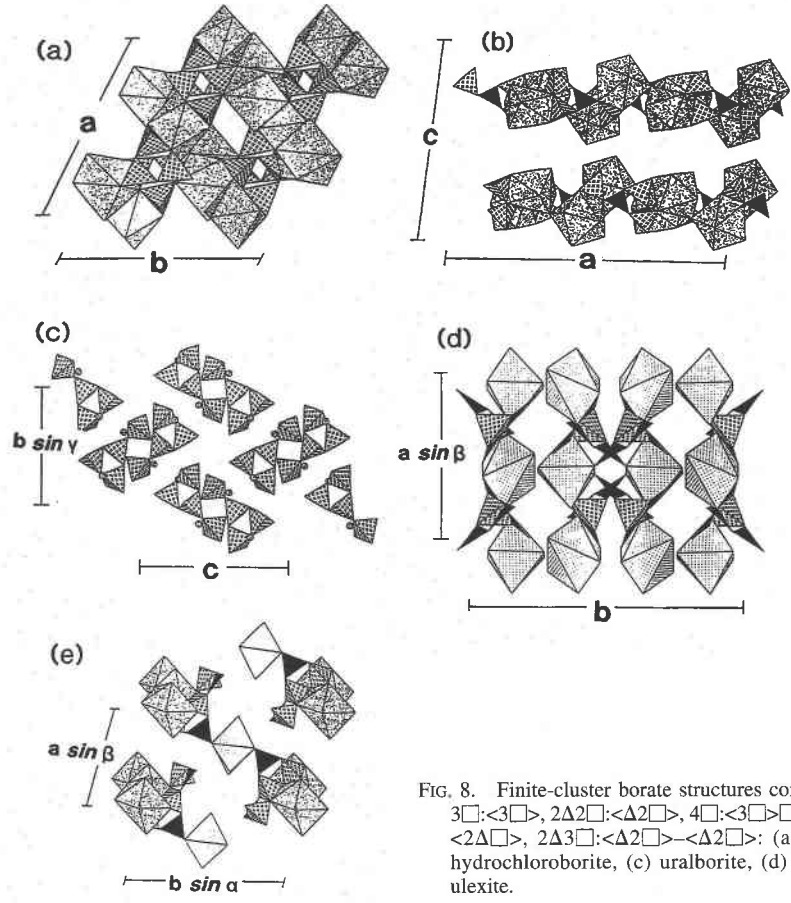

FIG. 8. Finite-cluster borate structures containing the *FBB*s 3□:<3□>, 2Δ2□:<Δ2□>, 4□:<3□>□, 4Δ1□:<2Δ□>–<2Δ□>, 2Δ3□:<Δ2□>–<Δ2□>: (a) nifontorite, (b) hydrochloroborite, (c) uralborite, (d) sborgite, and (e) ulexite.

FBB = 4□:<3□>□

This *FBB* (Fig. 5g) is a <3□> ring decorated with an additional (BO_4) group and occurs only in uralborite, $Ca_2[B_4O_4(OH)_8]$ (Fig. 8c). There are two distinct Ca atoms; one is coordinated by two O atoms and six (OH) groups, and the other is coordinated by three O atoms and five (OH) groups. The ($Ca\phi_8$) polyhedra share edges to form dimers that join with the <3□>□ decorated rings to form a heteropolyhedral framework. There is extensive H-bonding that further strengthens linkage across the large cavities in the structure.

FBB = 4Δ1□:<2Δ□>–<2Δ□>

This *FBB* (Fig. 5h) consists of two <2Δ□> rings that link *via* a common ($B\phi_4$) tetrahedron. It occurs as an isolated cluster in sborgite, $Na[B_5O_6(OH)_4](H_2O)_3$, and also in larderellite, where it polymerizes to form chains. In sborgite, there are two distinct Na atoms: one is coordinated by two (OH) groups and four (H_2O) groups, and the other is coordinated by two (OH) groups, two (H_2O) groups at 2.298 Å and a further two (H_2O) groups at 2.998 Å (Merlino & Sartori 1972). The ($Na\phi_6$) polyhedra and the <2Δ□>– <2Δ□> clusters link to form a three-dimensional network (Fig. 8d) that is strengthened by extensive H-bonding involving both direct OH...O interaction between borate clusters and interactions involving the (H_2O) group.

FBB = 2Δ3□:<Δ2□>–<Δ2□>

This *FBB* occurs in the finite-cluster mineral ulexite, as well as in polymerized form: chains in probertite and sheets in the structures of tuzlaite and the hilgardite polymorphs (see below). The *FBB* (Fig. 5i) consists of two ($B\phi_3$) groups and three ($B\phi_4$) groups that link by sharing corners to form two <Δ2ϕ> rings that fuse through a common ($B\phi_4$) group. In ulexite, $NaCa[B_5O_6(OH)_6](H_2O)_5$, there is one distinct Ca cation coordinated by three O atoms, three (OH) groups and two (H_2O) groups, and one distinct Na cation coordinated by two (OH) groups and four (H_2O) groups. The ($Na\phi_6$) octahedra form edge-sharing [$Na\phi_4$] chains, and the ($Ca\phi_8$) polyhedra share edges to form chains, both extending along the *c* axis (seen end-on in Fig. 8e). These chains link the polyborate anions into sheets parallel to (110), and these sheets are linked *via* H bonding.

FBB = 2Δ2□:<Δ2□>=<Δ2□>

The <Δ2□> ring is the dominant motif for the isolated-ring structures of this class (Fig. 5d) and, in accord with this, also the dominant component for the dimerized-ring structures of this class (Fig. 5j). In addition to five isolated-cluster structures, the *FBB* also polymerizes to form a framework in diomignite. Borax, $Na_2[B_4O_5(OH)_4](H_2O)_8$, has two distinct Na atoms, each of which is [6]- coordinated by (H_2O) groups. The ($Na\phi_6$) polyhedra share edges to form chains that are cross-linked by the <Δ2□>=<Δ2□> clusters into heteropolyhedral sheets parallel to {100} (Fig. 9a). These sheets are linked by an extensive network of H-bonds.

In tincalconite, $Na_2[B_4O_5(OH)_4](H_2O)_3$, there are three crystallographically distinct Na cations, all of which are in octahedral coordination by (OH) and (H_2O). The octahedra share edges and corners to form a discontinuous sheet parallel to (001) that is linked to adjacent sheets by edge-sharing of octahedra out of the plane of the sheet (Fig. 9b). The resultant framework has large interstices that contain the <Δ2□>=<Δ2□> clusters, and there is no interstitial H_2O. The structure shows prominent compositional layering and has strong affinities with the structure of borax (Fig. 9a). At 20–25°C and 60% relative humidity, borax and tincalconite convert to one another rapidly and reversibly (Christ & Garrels 1959).

In hungchaoite, $Mg[B_4O_5(OH)_4](H_2O)_7$, there is one unique Mg atom that is coordinated by one (OH) group and five (H_2O) groups. The resulting ($Mg\phi_6$) octahedron links by corner-sharing to a ($B\phi_4$) group of a <Δ2□>=<Δ2□> cluster (Fig. 9c). The resultant $Mg[B_4O_5(OH)_4](H_2O)_5$ cluster is neutral, and links to other clusters by direct H-bonding and by a H-bond network involving the two additional interstitial (H_2O) groups.

Fedorovskite, $Ca_2Mg_2(OH)_4[B_4O_7(OH)_2]$, and roweite, $CaMn^{2+}(OH)_4[B_4O_7(OH)_2]$, are isostructural minerals. In roweite, there are three unique Mn atoms; one is coordinated by four O atoms and two (OH) groups, one is coordinated by two O atoms and four (OH) groups, and the third is coordinated by six (OH) groups. The octahedra share *cis* edges to form [$M\phi_4$] chains that extend along [010], and these chains link together by sharing opposing apical vertices to form an open sheet of octahedra that resembles a distorted [$M\phi_3$] chequerboard; these sheets are cross-linked by <Δ2□>=<Δ2□> clusters (Fig. 9d) in the [001] direction. There is one unique Ca atom occupying the interstices of this framework; it is coordinated by three O atoms and five (OH) groups.

FBB = 3Δ3□:[ϕ]<Δ2□> | <Δ2□> | <Δ2□> |

This *FBB* (Fig. 5k) consists of three <Δ2□> rings that link to a common central anion through their tetrahedrally coordinated B atoms. It occurs in three isolated-cluster minerals, mcallisterite, aksaite and rivadavite, as well as in polymerized form: chains in aristarainite and sheets in tunellite and nobleite (see below). In mcallisterite, $Mg_2[B_6O_7(OH)_6]_2(H_2O)_9$, there is one unique Mg cation that is octahedrally coordinated by three (OH) and three (H_2O) groups. This octahedron links to three tetrahedra of the [ϕ]<Δ2□> | <Δ2□> | <Δ2□> | cluster by sharing corners (Fig. 10a). The resulting

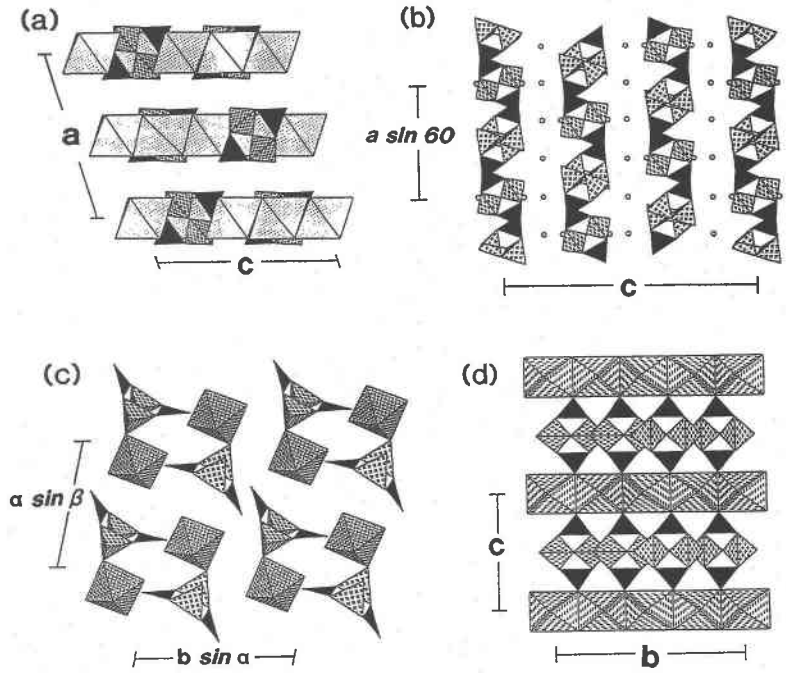

FIG. 9. Finite-cluster borate structures containing the *FBB* 2Δ2□:<Δ2□>=<Δ2□>: (a) borax, (b) tincalconite, (c) hungchaoite, and (d) roweite.

$Mg[B_6O_7(OH)_6]$ finite clusters are linked solely by H-bonding both directly from cluster to cluster and indirectly *via* interstitial (H_2O) groups.

Aksaite, $Mg[B_6O_7(OH)_6](H_2O)_2$, contains the same $Mg[B_6O_7(OH)_6]$ clusters as mcallisterite, but the lower hydration state (four H_2O as compared to nine H_2O in mcallisterite) indicates a higher connectivity in aksaite than in mcallisterite. In aksaite, the $Mg[B_4O_7(OH)_7]$ clusters link by sharing one vertex between an ($Mg\phi_6$) group of one cluster and a ($B\phi_3$) group of the next cluster to form chains extending along [001] (Fig. 10b). The chains are linked directly *via* H-bonds; there are no interstitial (H_2O) groups as in mcallisterite.

Complete details of the structure of rivadavite, $Na_6Mg[B_6O_7(OH)_6]_4(H_2O)_{10}$, are not available, but a preliminary report (Dal Negro & Ungaretti 1973) shows the presence of [ϕ]<Δ2□> | <Δ2□> | <Δ2□> | clusters linked into a framework by [6]-coordinated Mg and [6]-coordinated Na, with only one interstitial (H_2O) group present.

FBB = 12Δ3□:3(<2Δ□>–<2Δ□>)

Ammonioborite, $(NH_4)_3[B_{15}O_{20}(OH)_8](H_2O)_4$, is the only mineral with this very complex *FBB*. Two <2Δ□> rings link *via* a common (BO_4) group, and then three of these units link by sharing two triangular vertices to form a large and very flexible *FBB*, $[B_{15}O_{20}(OH)_8]$ (Fig. 5l). These clusters are linked *via* H-bonding involving interstitial (NH_4) groups, and the complete structure has strong compositional layering (Fig. 10c).

STRUCTURES BASED ON INFINITE CHAINS OF POLYHEDRA

There are seven distinct types of cluster in this class, and these may be divided into six sets: (1) B:B, (2) 3B:<3B>, (3) 5B:<3B>–<3B>, (4) 6B:<3B>–<3B>B, (5) 7B:<3B>–<3B>–<3B>, and (6) 6B:[ϕ]<3B> | <3B> | <3B> |. All but one of the sets involve a three-member ring of polyhedra. The minerals in this class are listed in Table 3, and the clusters are illustrated in Figure 11.

FBB = 1□:□

This *FBB* occurs in vimsite, $Ca[B_2O_2(OH)_4]$, as a single (BO_4) group (Fig. 11a) that polymerizes by sharing two vertices with adjacent (BO_4) groups to form a pyroxene-like chain that extends in the [001] direction. These chains are cross-linked into a heteropolyhedral framework by columns of ($Ca\phi_8$) polyhedra that also extend parallel to [001] (Fig. 12a).

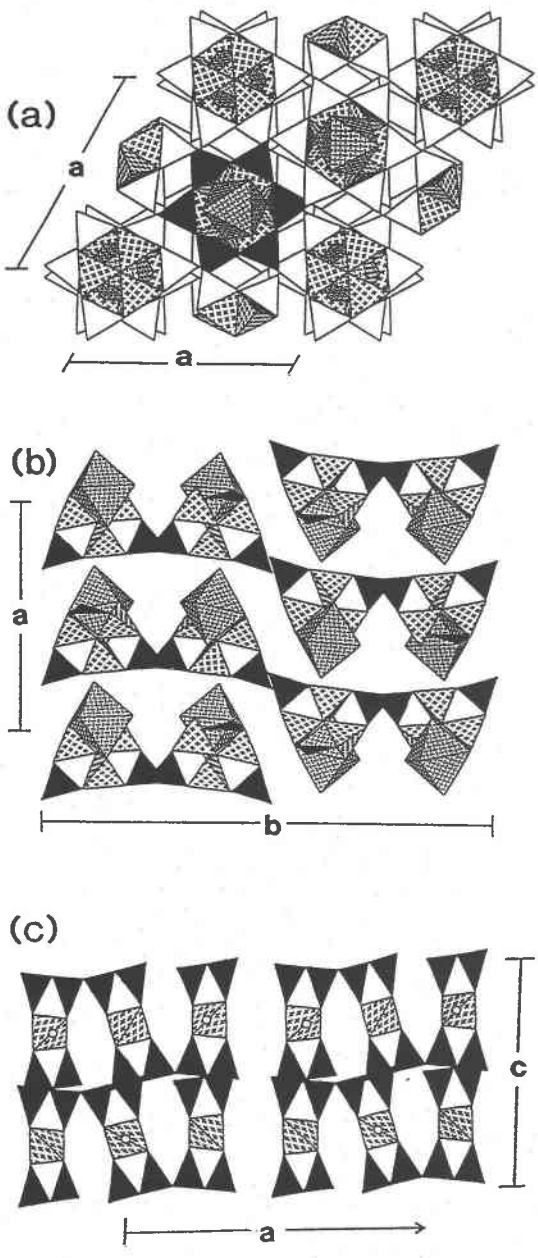

FIG. 10. Finite-cluster borate structures containing the *FBB*s $3\Delta3\square$:[ϕ]<$\Delta2\square$> | <$\Delta2\square$> | <$\Delta2\square$> | and $12\Delta3\square$:3(<$2\Delta\square$>–<$2\Delta\square$>): (a) mcallisterite, most BO_3 triangles are unshaded here for clarity, (b) aksaite, and (c) ammonioborite.

FBB = *1*$\Delta2\square$:<$\Delta2\square$>

This *FBB* (Fig. 11b) is quite common; it occurs in six finite-cluster structures (above) and in polymerized form as chains in the structures of colemanite, calciborite and hydroboracite (Table 3). In colemanite, $Ca[B_3O_4(OH)_3](H_2O)$, <$\Delta2\square$> rings share two vertices between triangles and tetrahedra of adjacent rings to form a chain extending along [100]. There is one unique Ca atom coordinated by eight anions in an irregular dodecahedral arrangement. The ($Ca\phi_8$) polyhedra share corners to form chains parallel to [100] (Fig. 12b). The [$Ca\phi_7$] chains cross-link the borate chains into a heteropolyhedral sheet of composition $[Ca_2B_3O(OH)(H_2O)]$ parallel to (010). These sheets, seen "edge-on" in Figure 12b, link *via* corner-sharing between (BO_4) tetrahedra and ($Ca\phi_8$) dodecahedra, and through an extensive network of H-bonds.

In calciborite, $Ca[B_2O_4]$, <$\Delta2\square$> rings link *via* common (BO_4) groups to form $[^{[3]}B^{[4]}B\phi_4]$ chains extending along [001] (Fig. 12c). The single Ca atom is coordinated by eight anions in a dodecahedral arrangement, and the resulting ($Ca\phi_8$) polyhedra link to form columns along [001]. Each column of dodecahedra is surrounded by six borate chains, and these link directly to form a heteropolyhedral framework.

Hydroboracite, $CaMg[B_3O_4(OH)_3](H_2O)_3$, consists of <$\Delta2\square$> rings that link through sharing triangle and tetrahedron vertices to form chains parallel to the *c* direction (Fig. 12d). There is a single Mg cation that is octahedrally coordinated by two (OH) groups and four (H_2O) groups, and the $Mg\phi_6$ octahedra link *via* sharing of *trans* vertices to form an [$Mg\phi_5$] chain, also extending in the *c* direction. Each [$Mg\phi_5$] chain is flanked by two borate chains (Fig. 12d). There is one unique Ca cation coordinated by eight anions in a dodecahedral arrangement. The ($Ca\phi_8$) dodecahedra polymerize to form chains parallel to *c*, and the borate chains link the [$Mg\phi_5$] and [$Ca\phi_7$] chains into a heteropolyhedral framework.

FBB = *4*$\Delta1\square$:<$2\Delta\square$>–<$2\Delta\square$>

This FBB (Fig. 11c) consists of pairs of <$2\Delta\square$> rings that link through a common (BO_4) group. It is uncommon, and occurs in the finite-cluster mineral sborgite, as well as polymerized to form chains in larderellite. In larderellite, $(NH_4)[B_5O_7(OH)_2](H_2O)$, the *FBB*s link through a triangle vertex to form a complex modulated chain extending along the *b* axis (Fig. 12e); the chain resembles the complex 3{<$2\Delta\square$>–<$2\Delta\square$>} cluster in ammonioborite. These chains are linked *via* H-bonds involving interstitial (NH_4) and (H_2O) groups. From the view in Figure 12e, it appears that individual <$2\Delta\square$>–<$2\Delta\square$> groups polymerize only by sharing two triangle vertices, but further linkage is provided by H-bonds between the (OH) groups of each ($B\phi_3$) triangle.

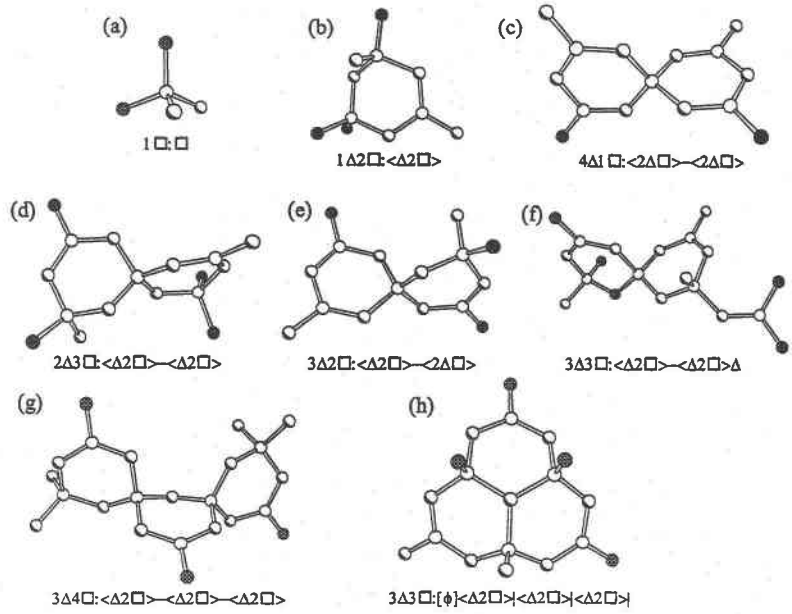

FIG. 11. The eight distinct clusters that occur as *FBB*s in the chain-borate minerals.

FBB = $2\Delta3\square$:$<\Delta2\square>$–$<\Delta2\square>$

This *FBB* (Fig. 11d) consists of two $<\Delta2\square>$ rings that link through a shared ($B\phi_4$) tetrahedron. It occurs in the finite-cluster mineral ulexite, and is polymerized to form chains in probertite, sheets in tuzlaite, and frameworks in the hilgardite polymorphs. In probertite, $NaCa[B_5O_7(OH)_4](H_2O)_3$, the *FBB*s link by sharing a vertex between ($B\phi_3$) and ($B\phi_4$) groups to form an infinite chain extending along [001], with chains adjacent along [010] pointing in opposing directions (Fig. 12f). The Ca atom is coordinated by five O atoms, three (OH) groups and an (H_2O) group, and the Na atom is coordinated by one O atom, two (OH) groups and three (H_2O) groups. Two ($Ca\phi_9$) polyhedra share an edge to form a dimer, and each end of the dimer shares an edge with an ($Na\phi_6$) polyhedron to form a large-cation tetramer. These tetramers cross-link the borate chains that weave between them, and this linkage is strengthened by a network of H-bonds involving both (OH) and (H_2O) groups.

TABLE 3. BORATE MINERALS BASED ON INFINTE CHAINS OF $B\Phi_3$ AND $B\Phi_4$ POLYHEDRA

Polyhedra	Name	Connectivity	Formula	*a* (Å)	*b* (Å)	*c* (Å)	β (°)	Sp. Gr.	Ref.	Fig.
1□	vimsite	□	$Ca[B_2O_2(OH)_4]$	10.026(2)	4.440(1)	9.558(3)	–	*B2/b*	(1)	12a
1Δ2□	colemanite	⟨Δ2□⟩	$Ca[B_3O_4(OH)_3](H_2O)$	8.712(2)	11.247(3)	6.091(1)	110.12(2)	$P2_1/a$	(2)	12b
1Δ2□	calciborite	⟨Δ2□⟩	$Ca[B_2O_4]$	8.38	13.82	5.006	–	*Pccn*	(3)	12c
1Δ2□	hydroboracite	⟨Δ2□⟩	$CaMg[B_3O_4(OH)_3](H_2O)_3$	11.769(2)	6.684(2)	8.235(4)	102.59(2)	*P2/c*	(4)	12d
4Δ1□	larderellite	⟨2Δ□⟩-⟨2Δ□⟩	$(NH_4)[B_5O_7(OH)_2](H_2O)$	9.47	7.63	11.65	97.08	$P2_1/c$	(5)	12e
2Δ3□	probertite	⟨Δ2□⟩-⟨Δ2□⟩	$NaCa[B_5O_7(OH)_4](H_2O)_3$	6.588(1)	12.560(2)	13.428(2)	99.97(1)	$P2_1/c$	(6)	12f
3Δ2□	ezcurrite	⟨Δ2□⟩-⟨2Δ□⟩	$Na_2[B_5O_7(OH)_3](H_2O)_2$	8.598(2)	9.570(2)	6.576(2)	107.50(5)	$P\bar{1}$	(7)	13a
3Δ3□	kaliborite	⟨Δ2□⟩-⟨Δ2□⟩Δ	$Kmg_2H[B_8O_8(OH)_5]_2(H_2O)_4$	18.572(6)	8.466(3)	14.689(5)	100.02(3)	*C2/c*	(8)	13b
3Δ4□	kernite	⟨Δ2□⟩-⟨Δ2□⟩-⟨Δ2□⟩	$Na_2[B_4O_6(OH)_2](H_2O)_3$	7.0172(2)	9.1582(2)	15.6774(5)	108.861(2)	$P2_1/c$	(9)	13c
3Δ3□	aristarainite	[ϕ]⟨Δ2□⟩|⟨Δ2□⟩|⟨Δ2□⟩|	$Na_2Mg[B_8O_8(OH)_4]_2(H_2O)_4$	18.886(4)	7.521(2)	7.815(1)	97.72(1)	$P2_1/a$	(10)	13d,e

vimsite: γ = 91.32(2)°; ezcurrite: α=102.75(5)°; γ=71.52(5)°

(1) Simonov *et al.* (1976c), (2) Burns & Hawthorne (1993a), (3) Egorov-Tismenko *et al.* (1980), (4) Sabelli & Stoppioni (1978), (5) Merlino & Sartori (1969), (6) Menchetti *et al.* (1982), (7) Cannillo *et al.* (1973), (8) Burns & Hawthorne (1994e), (9) Cooper *et al.* (1973), (10) Ghose & Wan (1977)

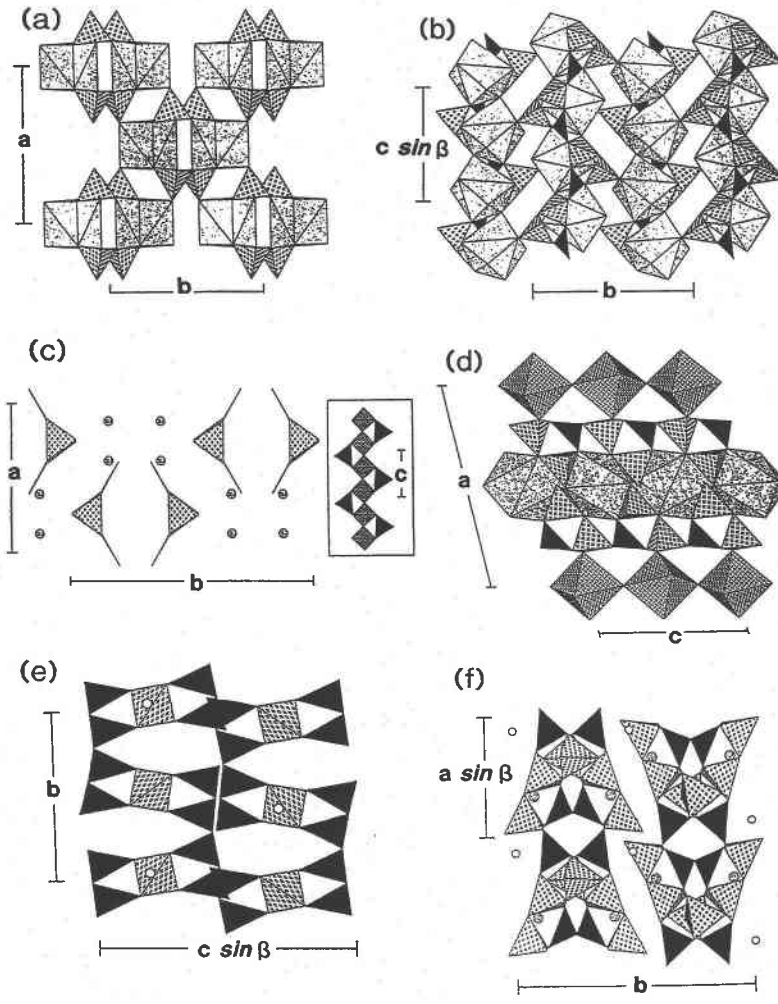

FIG. 12. Infinite-chain borate structures containing the *FBB*s 1□:□, 1Δ2□:<Δ2□>, 4Δ1□:<2Δ□>–<2Δ□>, and 2Δ3□:<Δ2□>–<Δ2□>: (a) vimsite, (b) colemanite, (c) calciborite, (d) hydroboracite, (e) larderellite, and (f) probertite.

FBB = *3Δ2□:<Δ2□>–<2Δ□>*

This *FBB* (Fig. 11e) has two different types of rings, <2Δ□> and <Δ2□> that link through a common tetrahedron. It is a common *FBB* that occurs polymerized to form chains in ezcurrite, as well as sheets in several structures (see below). In ezcurrite, $Na_2[B_4O_5(OH)_3](H_2O)_2$, the *FBB* shares two vertices between tetrahedra and triangles of adjacent clusters to form a chain parallel to the *c* axis (Fig. 13a). There are two distinct Na atoms in ezcurrite, one is [6]-coordinated by two O atoms, two (OH) groups and two (H_2O) groups, and one is [7]-coordinated by five O atoms, one (OH) group and one (H_2O) group. Pairs of ($Na\phi_7$) polyhedra share an edge to form an $[Na_2\phi_{12}]$ dimer, and pairs of ($Na\phi_6$) polyhedra share an edge to form an $[Na_2\phi_{10}]$ dimer. These dimers link by sharing vertices to form chains extending along [111]. The skewed chains link by sharing edges and vertices to form an extremely complex arrangement (Fig. 13a) that is further linked by a network of H-bonds.

FBB = *3Δ3□:<Δ2□>–<Δ2□>Δ*

This *FBB* (Fig. 11f) occurs only in kaliborite, $KMg_2H[B_6O_8(OH)_5]_2(H_2O)_4$, and is a decorated variety of the *FBB* in probertite: two <Δ2□> rings link through a common ($B\phi_4$) group, and an additional ($B\phi_3$) group is attached to a tetrahedron vertex. These clusters link by sharing vertices between triangles and tetrahe-

dra to form convoluted chains extending along [010] (Fig. 13b). The rigidity of the chain is reinforced by ($Mg\phi_6$) octahedra; each octahedron shares four vertices with borate polyhedra of the chain, the remaining pair of anions being interstitial (H_2O) groups. These heteropolyhedral chains are linked *via* interstitial [8]-coordinated K cations, each of which links to four separate chains. A complex network of H-bonds provides further linkage between the chains.

FBB = $3\Delta4\square$:<$\Delta2\square$>–<$\Delta2\square$>–<$\Delta2\square$>

This *FBB* (Fig. 11g) occurs only in kernite, $Na_2[B_4O_6(OH)_2](H_2O)_3$, and consists of a <$\Delta2\square$> ring that links to form a chain along [010] *via* sharing of a common tetrahedron between adjacent rings. There are two distinct Na sites; Na(1) is coordinated by five O atoms and one (H_2O) group, and Na(2) is coordinated by two O atoms and three (H_2O) groups. All (H_2O) groups are bonded to Na atoms, and the borate chains (Fig. 13c) are linked by both Na atoms and a complex network of H bonds.

FBB = $3\Delta3\square$:[ϕ]<$\Delta2\square$> | <$\Delta2\square$> | <$\Delta2\square$> |

This *FBB* (Fig. 11h) consists of three <$\Delta2\square$> rings that link to a central anion ([ϕ] in the *FBB* descriptor). It is a common *FBB* that occurs in the isolated-cluster minerals mcallisterite, aksaite and rivadavite, as well as polymerized to form chains in aristarainite and sheets in tunellite and nobleite. This *FBB* polymerizes to other *FBB*s in aristarainite, $Na_2Mg[B_6O_8(OH)_4]_2(H_2O)_4$, by linkage between ($B\phi_3$) and ($B\phi_4$) groups to form chains parallel to the *b*-axis (Fig. 13d). These chains are cross-linked into sheets parallel to (001) by ($Mg\phi_6$) octahedra (Fig. 13e), and these sheets are linked into a three-dimensional arrangement by ($Na\phi_5$) polyhedra and a network of H-bonds.

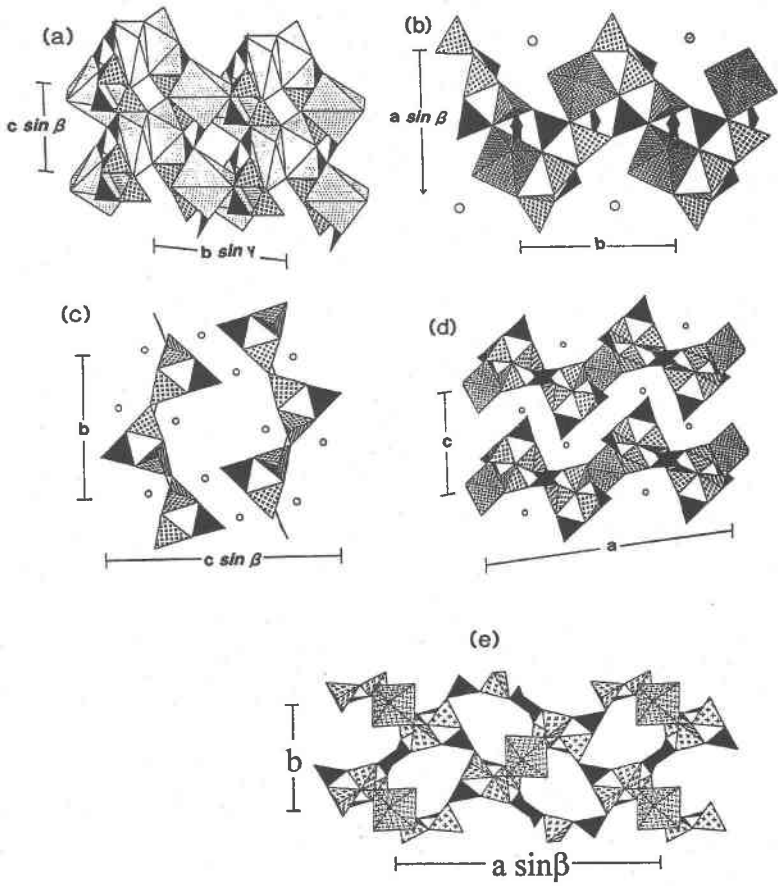

FIG. 13. Infinite-chain borate structures containing the *FBB*s $3\Delta2\square$:<$\Delta2\square$>–<$2\Delta\square$>, $3\Delta3\square$:<$\Delta2\square$>–<$\Delta2\square$>Δ, and $3\Delta4\square$:<$\Delta2\square$>–<$\Delta2\square$>–<$\Delta2\square$>: (a) ezcurrite, (b) kaliborite, (c) kernite, (d) aristarainite, and (e) aristarainite.

Structures Based on Infinite Sheets of Polyhedra

There are nine distinct types of clusters in this class, and these may be divided into eight sets: (1) 5B:<3B>–<3B>, (2) 6B:[ϕ]<3B> | <3B> | <3B> | , (3) 8B:[ϕ]<3B> | <3B> | <3B> | 2B, (4) 14B:[ϕ]<3B> | <3B> | <3B> | –[ϕ]<3B> | <3B> | <3B> | 2B, (5) 6B:<3B>=<4B>=<3B>, (6) 8B:<6B>=<4B>, (7) 11B:B<3B>–<3B>–<3B>–<3B>B, and (8) 12B:<12B>. All but one of the sets involve a three-membered ring of polyhedra. The minerals in this class are listed in Table 4, and the clusters are illustrated in Figure 14.

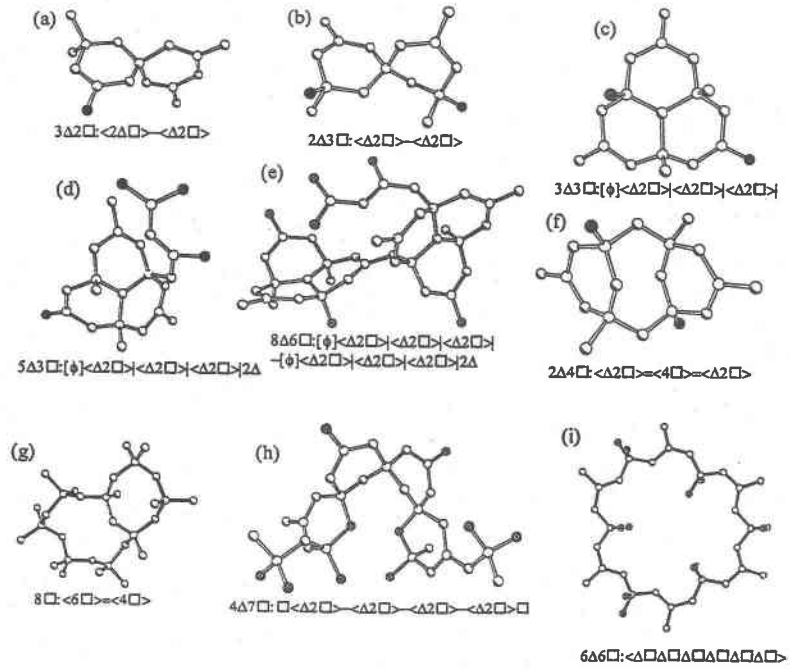

FIG. 14. The nine distinct clusters that occur as *FBB*s in the sheet-borate minerals.

TABLE 4. BORATE MINERALS BASED ON INFINITE SHEETS OF $B\Phi_3$ OR $B\Phi_4$ POLYHEDRA

Polyhedra	Name	Connectivity	Formula	*a* (Å)	*b* (Å)	*c* (Å)	β (°)	Sp.Gr.	Ref.	Fig.
3Δ2□	biringuccite	⟨Δ2□⟩-⟨2Δ□⟩	$Na_3[B_5O_8(OH)](H_2O)$	11.1955	6.5607	20.7566	93.891	$P2_1/c$	(1)	15a,b
3Δ2□	nasinite	⟨Δ2□⟩-⟨2Δ□⟩	$Na_2[B_5O_8(OH)](H_2O)_2$	12.015(2)	6.518(1)	11.173(1)	–	$Pna2_1$	(2)	15c
3Δ2□,1Δ	gowerite	⟨Δ2□⟩-⟨2Δ□⟩,Δ	$Ca[B_5O_8(OH)][B(OH)_3](H_2O)_3$	12.882(4)	16.360(7)	6.558(4)	121.62(5)	$P2_1/a$	(3)	15d
3Δ2□,1Δ	veatchite	⟨Δ2□⟩-⟨2Δ□⟩,Δ	$Sr_2[B_5O_8(OH)]_2[B(OH)_3](H_2O)$	20.860(5)	11.738(3)	6.625(2)	92.10(3)	Aa	(4)	15e
3Δ2□,1Δ	p-veatchite	⟨Δ2□⟩-⟨2Δ□⟩,Δ	$Sr_2[B_5O_8(OH)]_2[B(OH)_3](H_2O)$	6.70	20.80	6.60	119.25	$P2_1$	(5)	–
3Δ2□,1Δ	volkovskite	⟨Δ2□⟩-⟨2Δ□⟩,Δ	$KCa_4[B_5O_8(OH)]_4[B(OH)_3]_2Cl(H_2O)_4$	6.500	23.960	6.620	119.60	$P1$	(6)	15f
2Δ3□	tuzlaite	⟨Δ2□⟩-⟨Δ2□⟩	$NaCa[B_6O_9(OH)_2](H_2O)_3$	6.506(1)	13.280(3)	11.462(3)	92.97(2)	$P2_1/c$	(7)	16a,b
3Δ3□	nobleite	[ϕ]⟨Δ2□⟩|⟨Δ2□⟩|⟨Δ2□⟩|	$Ca[B_5O_9(OH)_2](H_2O)_3$	14.56(5)	8.02(2)	9.84(2)	111.8(2)	$P2_1/a$	(8)	–
3Δ3□	tunellite	[ϕ]⟨Δ2□⟩|⟨Δ2□⟩|⟨Δ2□⟩|	$Sr[B_6O_9(OH)_2](H_2O)_3$	14.415(3)	8.213(1)	9.951(2)	114.05(1)	$P2_1/a$	(9)	16c,d
5Δ3□	strontioborite	[ϕ]⟨Δ2□⟩|⟨Δ2□⟩|⟨Δ2□⟩|2Δ	$Sr[B_6O_{11}(OH)_4]$	9.909(5)	8.130(10)	7.623(1)	108.4(2)	$P2_1$	(10)	16e
8Δ6□	ginorite	[ϕ]⟨Δ2□⟩|⟨Δ2□⟩|⟨Δ2□⟩|-[ϕ]⟨Δ2□⟩|⟨Δ2□⟩|⟨Δ2□⟩|2Δ	$Ca_2[B_{14}O_{20}(OH)_6](H_2O)_5$	12.74(1)	14.36(2)	12.82(2)	100.77(3)	$P2_1/a$	(11)	–
8Δ6□	strontioginorite	[ϕ]⟨Δ2□⟩|⟨Δ2□⟩|⟨Δ2□⟩|-[ϕ]⟨Δ2□⟩|⟨Δ2□⟩|⟨Δ2□⟩|2Δ	$Sr_2[B_{14}O_{20}(OH)_6](H_2O)_5$	12.817(8)	14.488(8)	12.783(8)	101.42(8)	$P2_1/a$	(11)	17a
2Δ4□	fabianite	⟨Δ2□⟩=⟨4□⟩=⟨Δ2□⟩	$Ca_2[B_6O_{10}(OH)_2]$	6.593	10.488	6.365	113.38	$P2_1/a$	(12)	17b
8□	johachidolite	⟨6□⟩=⟨4□⟩	$Ca_3Al_2[B_6O_{14}]$	7.970	11.722	4.374	–	$Cnma$	(13)	17c
4Δ7□	preobrazhenskite	□⟨Δ2□⟩-⟨Δ2□⟩-⟨Δ2□⟩-⟨Δ2□⟩□	$Mg_3[B_{11}O_{15}(OH)_3]$	16.291(4)	9.181(2)	10.571(2)	–	$Pbcn$	(14)	17d
6Δ6□	brianroulstonite	<Δ□=>=	$Ca_4[B_5O_6(OH)_6](OH)Cl_2(H_2O)_4$	17.42(4)	8.077(5)	8.665(6)	121.48(7)	Pa	(15)	17e

volkovskite: α = 95.68°, γ = 90.59°

(1) Corazza *et al.* (1974), (2) Corazza *et al.* (1975), (3) Konnert *et al.* (1972), (4) Clark & Christ (1971): (5) Rumanova & Gandymov (1971), (6) Rastsvetaeva *et al.* (1992), (7) Bermanec *et al.* (1994), (8) Erd *et al.* (1961), (9) Burns & Hawthorne (1994a), (10) Brovkin *et al.* (1975), (11) Konnert *et al.* (1970a), (12) Konnert *et al.* (1970b), (13) Moore & Araki (1972b), (14) Burns & Hawthorne (1994b), (15) Grice *et al.* (1997)

FBB = $3\Delta 2\square$:<$\Delta 2\square$>–<$2\Delta\square$>

This *FBB* (Fig. 14a) has five [1]-coordinated anions, three of which are bonded to $^{[3]}$B and two of which are bonded to $^{[4]}$B. This is a common *FBB* that occurs polymerized to form chains in ezcurrite, as well as sheets in seven minerals. In nasinite and biringuccite, the basic $3\Delta 2\square$:<$2\Delta\square$>–<$\Delta 2\square$> *FBB* links to form a sheet by sharing two triangle vertices with two tetrahedron vertices of neighboring *FBB*s and two tetrahedron vertices with two triangle vertices of neighboring *FBB*s (Fig. 15a). In biringuccite, all the (BO_3) groups not involved with linkage between *FBB*s point one way (Fig. 15b), whereas in nasinite, the corresponding (BO_3) groups point in opposing directions in adjacent *FBB*s (Fig. 15c). Thus, the structural units in nasinite and biringuccite are geometrical isomers (Hawthorne 1983, 1985). There are four independent Na cations in biringuccite, $Na_2[B_5O_8(OH)](H_2O)$. Two of the independent Na cations are coordinated by eight and seven O and OH anions, respectively, all of which belong to the structural unit; the resultant coordination polyhedra share edges and corners to form chains. The other two Na atoms are coordinated by anions belonging to the structural unit and by interstitial (H_2O) groups, and are [7]- and [6]-coordinated, respectively. Two equivalent [7]-coordinated polyhedra share an edge to form a dimer, and these dimers bridge chains of ($Na\phi_8$) polyhedra to form sheets orthogonal to [100]. ($Na\phi_6$) polyhedra link these sheets to other chains of ($Na\phi_8$)

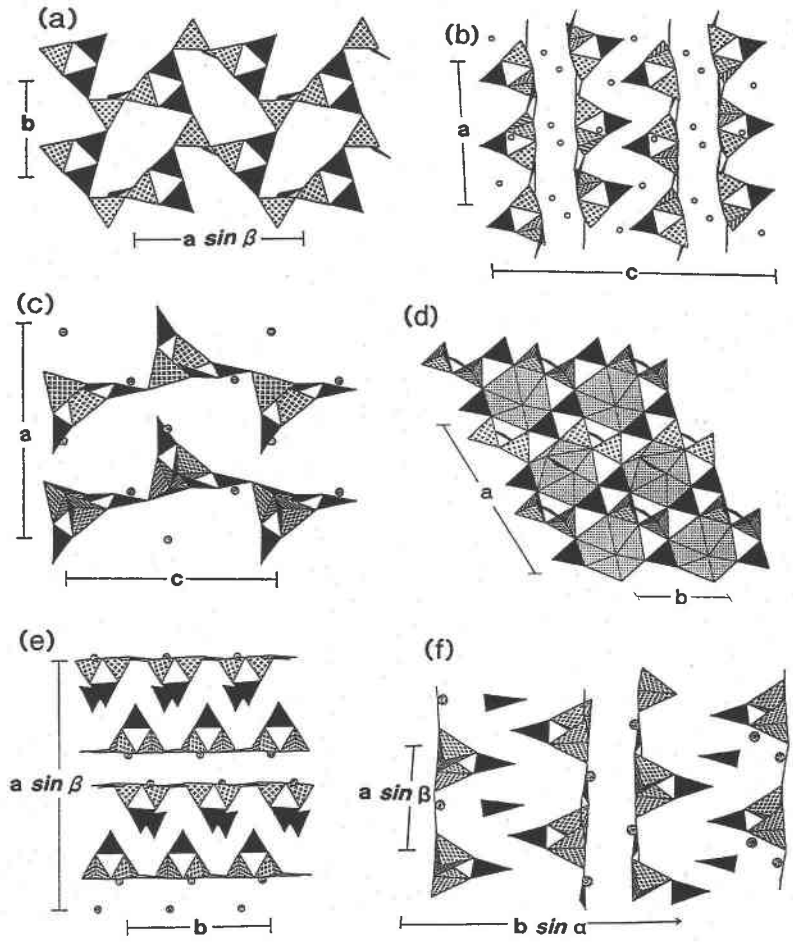

FIG. 15. Infinite-sheet borate minerals containing the *FBB*s $3\Delta 2\square$:<$\Delta 2\square$>–<$2\Delta\square$> and $3\Delta 2\square,1\Delta$:<$\Delta 2\square$>–<$2\Delta\square$>,Δ: (a) biringuccite, (b) biringuccite, (c) nasinite, (d) gowerite, (e) veachite, and (f) volkovskite.

polyhedra, forming a continuous framework that intercalates the $[B_5O_8(OH)]$ sheets. In nasinite, $Na_2[B_5O_8(OH)](H_2O)_2$, there are two independent Na cations, both of which are [8]-coordinated and link to interstitial (H_2O) groups. The ($Na\phi_8$) polyhedra share edges to form a framework that encloses the $[B_5O_8(OH)]$ sheets. The reason for the more complex arrangement of interstitial cations in biringuccite is related to the conformation of the borate sheets. In biringuccite (Fig. 15b), there are two types of interstitial space, one bounded by straight parallel sides and one bounded by zigzag parallel sides. In nasinite (Fig. 15c), there is only one type of interstitial space, bounded by the convoluted surface of the structural unit. Thus in biringuccite, the interstitial space occupied by Na and (H_2O) is far more varied in local environment, accounting for the more complicated array of interstitial species.

FBB = $3\Delta 2\square, 1\Delta$:<$\Delta 2\square$>–<$2\Delta\square$>,$\Delta$

This *FBB* consists of two separate (*i.e.*, not linked) units, a sheet that contains a <$\Delta 2\square$>–<$2\Delta\square$> cluster, and an isolated Δ group. There are four minerals with this combination of two *FBB*s: gowerite, veatchite, p-veatchite and volkovskite (Table 4). In gowerite, $Ca[B_5O_8(OH)][B(OH)_3](H_2O)_3$, the sheet of <$\Delta 2\square$>–<$2\Delta\square$> clusters is of the nasinite type (*cf.* Figs. 15c, d). There is one unique Ca site coordinated by nine anions, including one of the three distinct (H_2O) groups. The Ca atoms lie within the plane of the borate sheet (Fig. 15d), and the ($Ca\phi_9$) polyhedron shares an edge with the isolated ($B\phi_3$) group. The sheets stack along [010] and are linked solely by H-bonding, both directly and *via* the two additional interstitial (H_2O) groups that do not bond directly to any cation.

In veatchite and p-veatchite, $Sr_2[B_5O_8(OH)]_2[B(OH)_3](H_2O)$, the *FBB* <$\Delta 2\square$>–<$2\Delta\square$> connects to form a sheet of the biringuccite type (Fig. 15a), in which the neighboring <$\Delta 2\square$> groups within the same sheet point in the same direction, together with an isolated Δ group. In each structure, there are two distinct Sr sites, one of which is [10]-coordinated, and the other of which is [11]-coordinated. The Sr atoms lie in the plane of the borate sheets (Fig. 15e) and link two sheets together to form a thick slab that has the bulk composition of the mineral; these slabs are then linked together by H-bonding. The difference between the structures of veatchite and p-veatchite involves only a slight shift in the relative positions of adjacent sheets (Clark & Christ 1971) that result from the difference in space group: *Aa* for veatchite (Clark & Christ 1971) and *P*2 for p-veatchite (Rumanova & Gandymov 1971).

In volkovskite, $KCa_4[B_5O_8(OH)]_4[B(OH)_3]_2Cl(H_2O)_4$, the structural unit consists of two unconnected parts, a biringuccite-like sheet of <$\Delta 2\square$>–<$2\Delta\square$> clusters and an isolated Δ group. This arrangement is somewhat similar to those of veatchite and p-veatchite. However, the Δ groups point in opposing directions in volkovskite (Fig. 15f), whereas they all point the same way in veatchite and p-veatchite (Fig. 15e). The Ca atoms occur in the plane of the sheets of <$\Delta 2\square$>–<$2\Delta\square$> clusters and link back-to-back sheets into thick slabs (Fig. 15f), as is the case for veachite and p-veatchite. However, the additional K cation is displaced from the plane of the sheet and links adjacent slabs together, supplemented by extensive H-bonding.

FBB = $2\Delta 3\square$:<$\Delta 2\square$>–<$\Delta 2\square$>

This *FBB* (Fig. 14b) occurs in the finite-cluster mineral ulexite, as well as polymerized to form chains in probertite, sheets in tuzlaite, and frameworks in the hilgardite polymorphs. It consists of two <$\Delta 2\square$> rings that link together through a common ($B\phi_4$) group. In tuzlaite, $NaCa[B_5O_8(OH)_2](H_2O)_3$, the *FBB* links to other clusters by sharing triangle vertices with neighboring tetrahedra and tetrahedron vertices with neighboring triangles to form a sheet perpendicular to [001] (Fig. 16a). In addition to the three-membered rings, there are prominent ten-membered rings that consist of alternating corner-sharing tetrahedra and triangles (Fig. 16b). Each ten-membered ring consists of four *FBB*s, and each *FBB* links in a topologically unique manner. As there is only one symmetrically unique *FBB* in the sheet, each *FBB* must belong to four ten-membered rings, and inspection of Figure 16b shows this to be the case. This topological diversity offers the possibility of extensive geometrical isomerism (Hawthorne 1983) in this particular type of sheet. The sheet is quite corrugated in both the *a* and *b* directions, and the corrugations of adjacent sheets intermesh (Fig. 16a). There is one Ca atom, coordinated by six O atoms and two (H_2O) groups, and one Na atom, coordinated by four O atoms and three (H_2O) groups. The ($Ca\phi_8$) and ($Na\phi_7$) polyhedra share a face to form a dimer, and adjacent dimers link through edge-sharing of like polyhedra to form chains approximately orthogonal to the borate sheets; Na atoms occur close to the plane of the borate sheet (Fig. 16a), whereas Ca atoms occupy a position intermediate between adjacent sheets.

FBB = $3\Delta 3\square$:[ϕ]<$\Delta 2\square$> | <$\Delta 2\square$> | <$\Delta 2\square$> |

This *FBB* (Fig. 14c) is quite common, and occurs in three finite-cluster minerals, as well as in polymerized linkages to form chains in aristarainite and sheets in nobleite and tunellite. Three <$\Delta 2\square$> rings link by sharing tetrahedra; each ring shares one tetrahedron with each of the other two rings. This produces a cluster with three triangles and three tetrahedra, and the tetrahedra all link together *via* a common vertex denoted by [ϕ] in the designation for the *FBB*. In the isostructural minerals tunellite, $Sr[B_6O_9(OH)_2](H_2O)_3$, and nobleite, $Ca[B_6O_9(OH)_2](H_2O)_3$, each *FBB* shares anions with four other *FBB*s, and each of these *FBB*s points in a direction opposite to that of the central *FBB*. This ar-

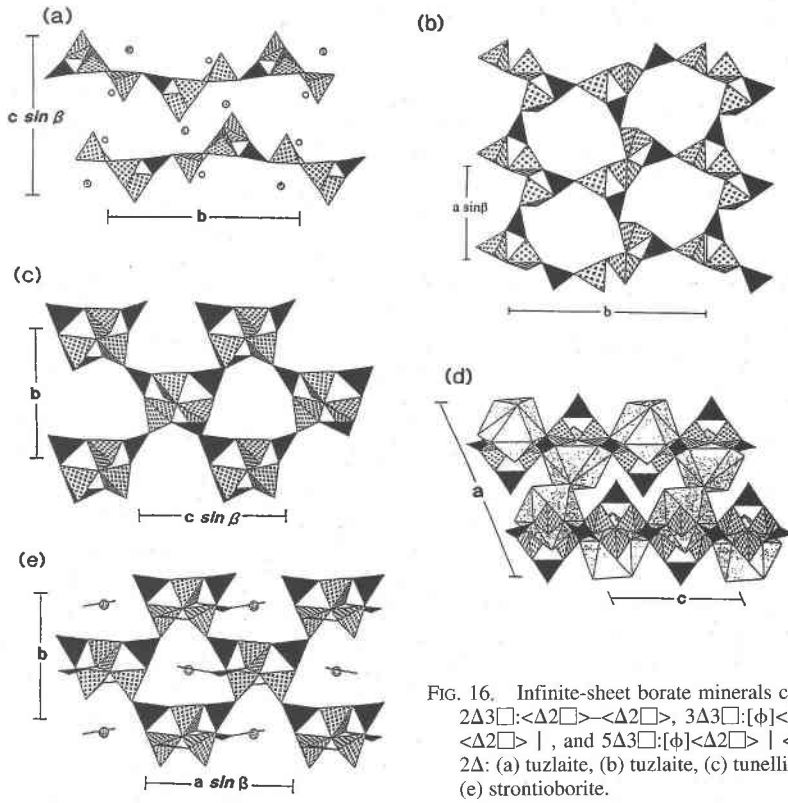

FIG. 16. Infinite-sheet borate minerals containing the *FBB*s 2Δ3□:<Δ2□>–<Δ2□>, 3Δ3□:[ϕ]<Δ2□> | <Δ2□> | <Δ2□> | , and 5Δ3□:[ϕ]<Δ2□> | <Δ2□> | <Δ2□> | 2Δ: (a) tuzlaite, (b) tuzlaite, (c) tunellite, (d) tunellite, and (e) strontioborite.

rangement results in sheets that contain alternating rows of *FBB*s, with all *FBB*s pointing either up (central row parallel to [001] in Fig. 16c) or down (peripheral rows parallel to [001] in Fig. 16c). Each *FBB* shares two tetrahedron vertices with two *FBB*s on one side, and two triangle vertices with two *FBB*s on the other side. This leaves vertices of one triangle and one tetrahedron that do not bridge between borate polyhedra. There is one unique Sr position that is coordinated by ten anions. The Sr cations are centered in the holes of the borate sheet (Fig. 16d) and do not link adjacent sheets directly. The linkage between adjacent sheets occurs *via* Sr–(H_2O)–Sr vertex-sharing, together with a network of H-bonds involving both (OH) and (H_2O) groups.

FBB = 5Δ3□:[ϕ]<Δ2□> | <Δ2□> | <Δ2□> | 2Δ

This *FBB* (Fig. 14d) occurs only in strontioborite, $Sr[B_8O_{11}(OH)_4]$, although it is similar to the *FBB* in tunellite and nobleite, and the finite-cluster minerals mcallisterite, aksaite and rivadavite. Three <Δ2□> rings link by sharing tetrahedra. Each ring shares one tetrahedron with the adjacent two rings, producing a cluster of three triangles and three tetrahedra in which the three tetrahedra link together *via* a common vertex, as is the case for the *FBB* in tunellite and nobleite (Fig. 14c). However, the *FBB* in strontioborite is decorated with a 2Δ cluster, a [B_2O_5] pyro-group similar to those found in the finite-cluster minerals suanite, száibélyite, sussexite and kurchatovite (Fig. 14d). The linkage of *FBB*s to form a sheet (Fig. 16e) is similar to that in tunellite (Fig. 16c). The strontioborite sheet shows the same alternating rows of *FBB* pointing in different directions (compare Figs. 16c, e), but this feature is exaggerated in strontioborite by the decoration of the sheet by the 2Δ cluster. The Sr cation is centered (in projection) in the holes of the borate sheet (Fig. 16e), and adjacent sheets are linked by Sr cations and by a network of H-bonds.

FBB = 8Δ6□:[ϕ]<Δ2□> | <Δ2□> | <Δ2□> | –[ϕ]<Δ2□> | <Δ2□> | <Δ2□ > | 2Δ

The isostructural minerals ginorite, $Ca_2[B_{14}O_{20}(OH)_6](H_2O)_5$, and strontioginorite, $Sr_2[B_{14}O_{20}(OH)_6](H_2O)_5$, have this *FBB*, which combines the *FBB* in nasinite and strontioborite, a [ϕ]<Δ2□> | <Δ2□> | <Δ2□> | cluster linked to its decorated analogue [ϕ]<Δ2□> | <Δ2□> | <Δ2□> | 2Δ (Fig. 14e). In the refined structure of strontioginorite (Konnert & Clark

1970), there are two distinct sites, one of which is occupied by Sr and the other of which is occupied by Ca. Sr is coordinated by six O atoms, two (OH) groups and two (H_2O) groups; Ca is coordinated by six O atoms, one (OH) group and one (H_2O) group. The Sr and Ca atoms are arranged in planes parallel to {010}, but do not link together directly; they bond to the *FBB*s to form very complex heteropolyhedral sheets parallel to {010} (Fig. 17a). These sheets are cross-linked solely by H-bonding; note that two (H_2O) groups do not link directly to any cations, but do play an important role in the H-bond network.

FBB = *2Δ4□:<Δ2□>=<4□>=<Δ2□>*

This *FBB* (Fig. 14f), known only in fabianite, $Ca_2[B_6O_{10}(OH)_2]$, consists of a four-membered ring of tetrahedra, <4□>, that shares two *trans* edges with two three-membered rings, <Δ2□>; the resulting cluster consists of four tetrahedra and two triangles. These clusters link by sharing two tetrahedron and two triangle vertices with adjacent clusters to form a sheet (Fig. 17b). The sheet is corrugated, and linkage of the *FBB*s produces ten-membered borate rings. There is one distinct Ca atom that is coordinated by six O atoms and two (OH) groups. The ($Ca\phi_8$) polyhedra share edges to form chains that extend along [100]. Rows of these chains occur between the borate sheets and bind them in stacks along [001], with additional inter-sheet linkage from H-bonds involving the OH anion.

FBB = *8□:<6□>=<4□>*

Johachidolite, $Ca_2Al_2[B_6O_{14}]$, is the only mineral that contains this *FBB*, which consists of a six-membered ring of tetrahedra that shares an edge with a four-membered ring of tetrahedra (Fig. 14g). The *FBB*s link by sharing edges between the six-membered rings and between the six- and four-membered rings, and by sharing vertices between six-membered rings and between four-membered rings (Fig. 17c) to form a sheet parallel to (001). The Al atom is centered in the four-membered ring and has octahedral coordination, and the Ca atom is centered in the six-membered ring and has [8]-coordination. Adjacent sheets are linked *via* both Al and Ca atoms.

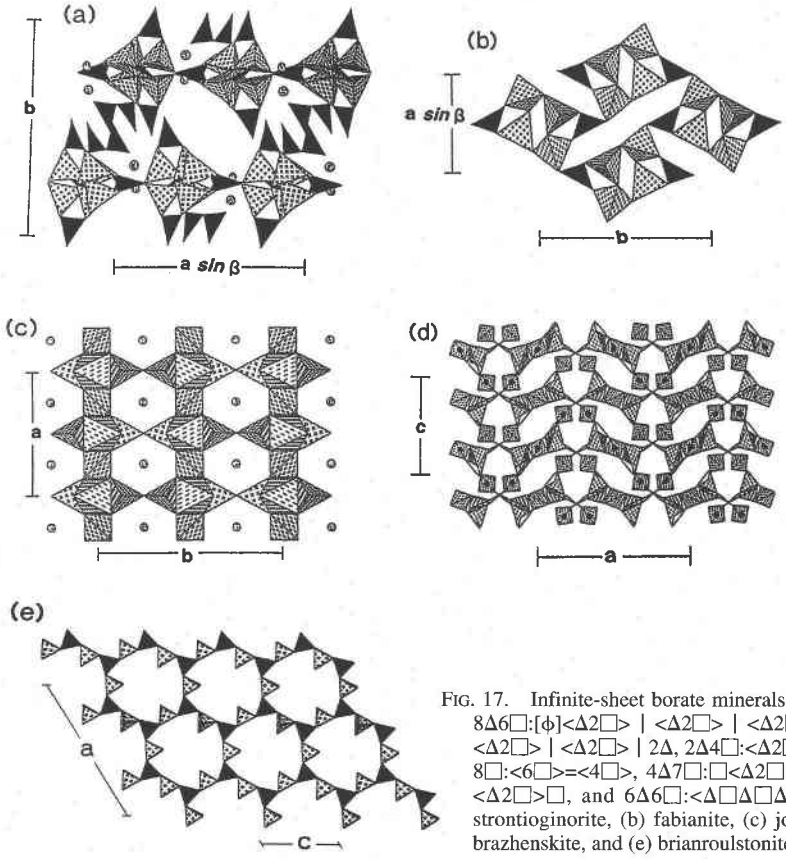

FIG. 17. Infinite-sheet borate minerals containing the *FBB*s 8Δ6□:[ϕ]<Δ2□> | <Δ2□> | <Δ2□> | – [ϕ]<Δ2□> | <Δ2□> | <Δ2□> | 2Δ, 2Δ4□:<Δ2□>= <4□>=<Δ2□>, 8□:<6□>=<4□>, 4Δ7□:□<Δ2□>–<Δ2□>–<Δ2□>–<Δ2□>□, and 6Δ6□:<Δ□Δ□Δ□Δ□Δ□Δ□>: (a) strontioginorite, (b) fabianite, (c) joachidolite, (d) preobrazhenskite, and (e) brianroulstonite.

FBB = 4Δ7□:□<Δ2□>–<Δ2□>–<Δ2□>–<Δ2□>□

Preobrazhenskite, $Mg_3[B_{11}O_{15}(OH)_9]$, is the only mineral that contains this *FBB*. It consists of four three-membered <Δ2□> rings, each of which links to one or two other rings *via* a common tetrahedron. The resulting arrangement is topologically linear, although the terminal ([1]-connected) rings are joined *via* a symmetrical H-bond, and this tetrameric group is decorated by the addition of a tetrahedron at each end (Fig. 14h). The *FBB* clusters link by sharing corners between triangles and tetrahedra to form a corrugated borate sheet parallel to (010) (Fig. 17d). There are two distinct Mg sites, each of which is octahedrally coordinated by both O and (OH) anions and links the sheets into a strongly bonded arrangement that is reinforced by extensive H-bonding.

FBB = 6Δ6□:<Δ□Δ□Δ□Δ□Δ□Δ□Δ□>

Brianroulstonite, $Ca_3[B_5O_6(OH)_6](OH)Cl_2(H_2O)_8$, is the only sheet mineral that contains this *FBB* (which also occurs in the framework minerals pringleite, ruitenbergite and penobsquisite). The *FBB* consists of a twelve-membered ring of alternating triangles and tetrahedra (Fig. 14i) that may be written in condensed form as 6Δ6□:<Δ□•>. The *FBB* clusters meld to form a sheet of twelve-membered rings, the centers of which define a 3^6 net (Fig. 17e). These sheets are linked through H-bonding, Ca and Cl atoms to form a sheet structure. The decorated sheets of the related framework borates form frameworks because the decorations (three-membered borate rings) promote direct linkage of the sheets to form frameworks.

Structures Based Upon Frameworks of Polyhedra

There are fifteen species (Table 5) that are based upon frameworks of borate polyhedra. There are seven distinct clusters that form *FBB*s (Fig. 18), and these may be divided into the following seven sets: (1) 3B:<3B>, (2) 4B:<3B>=<3B>, (3) 5B:<3B>–<3B>, (4) 4B:[ϕ] B | B | B | B |, (5) 7B:[ϕ]<3B> | <3B> | <3B> | B, (6) 15B:<B•>=<3B>B, and (7) 16B:<B•> = <3B>–<3B>.

FBB = 3□:<3□>

Metaborite, $[B_3O_3(OH)_3]$, is the only framework mineral with this FBB. The structure is based upon the *FBB* 3□:<3□> (Fig. 18a), which also occurs in the

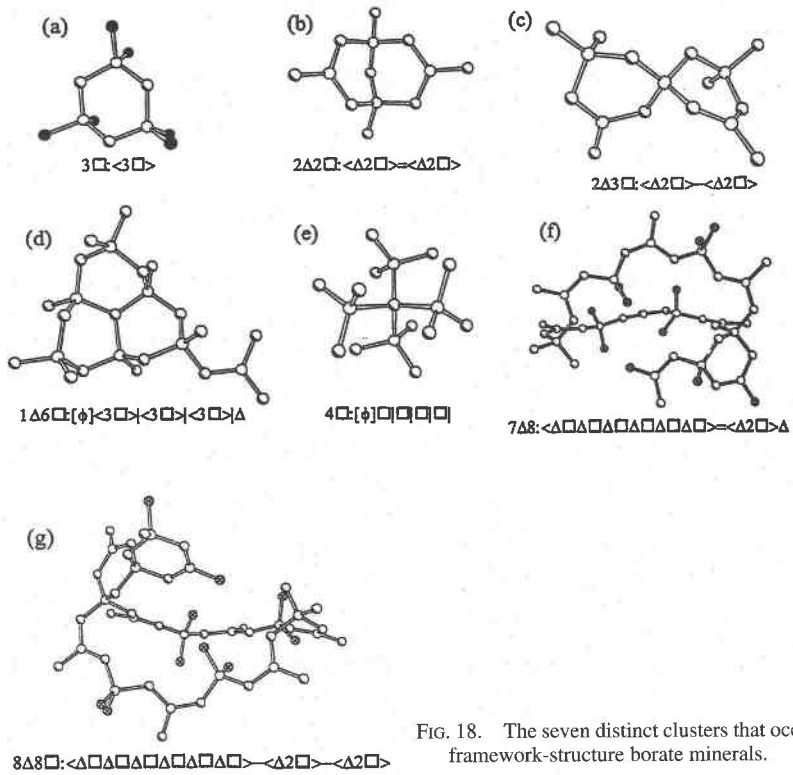

FIG. 18. The seven distinct clusters that occur as *FBB*s in the framework-structure borate minerals.

TABLE 5. BORATE MINERALS BASED ON INFINITE FRAMEWORKS OF $B\phi_3$ OR $B\phi_4$ POLYHEDRA

Polyhedra	Name	Connectivity	Formula	*a* (Å)	*b* (Å)	*c* (Å)	β (°)	Sp. Gr.	Ref.	Fig.
3□	metaborite	⟨3□⟩	$B_3O_3(OH)_3$	8.886(1)	–	–	–	$P\bar{4}3n$	(1)	–
2Δ2□	diomignite	⟨Δ2□⟩=⟨Δ2□⟩	$Li_2[B_4O_7]$	9.47	9.47	10.26	–	$I4_1cd$	(2)	19a
2Δ3□	hilgardite-1A	⟨Δ2□⟩-⟨Δ2□⟩	$Ca_2[B_5O_9]Cl(H_2O)$	6.452(1)	6.559(1)	6.286(1)	118.72(1)	$P1$	(3)	19b
2Δ3□	hilgardite-4M	⟨Δ2□⟩-⟨Δ2□⟩	$Ca_2[B_5O_9]Cl(H_2O)$	11.438(2)	11.318(2)	6.318(1)	90.06(1)	Aa	(4)	–
2Δ3□	hilgardite-3A	⟨Δ2□⟩-⟨Δ2□⟩	$Ca_6[B_5O_9]_3Cl_3(H_2O)_3$	17.495(4)	6.487(1)	6.313(1)	79.56(1)	$P1$	(5)	–
2Δ3□	tyretskite-1A	⟨Δ2□⟩-⟨Δ2□⟩	$Ca_2[B_5O_9](OH)(H_2O)$	6.44	6.45	6.41	60.3	–	(6)	–
1Δ6□	boracite (low)	[ϕ]⟨3□⟩|⟨3□⟩|⟨3□⟩|Δ	$Mg_3[B_6O_{10}][BO_3]Cl$	8.5496	8.5496	12.0910(9)	–	$Pca2_1$	(7)	19c
1Δ6□	chambersite	[ϕ]⟨3□⟩|⟨3□⟩|⟨3□⟩|Δ	$Mn_3[B_6O_{10}][BO_3]Cl$	8.68(1)	8.68(1)	12.26(1)	–	$Pca2_1$	(8)	–
1Δ6□	congolite	[ϕ]⟨3□⟩|⟨3□⟩|⟨3□⟩|Δ	$Fe_3[B_6O_{10}][BO_3]Cl$	8.622(1)	8.622(1)	21.054(5)	–	$R3c$	(7)	–
1Δ6□	ericaite	[ϕ]⟨3□⟩|⟨3□⟩|⟨3□⟩|Δ	$Fe_3[B_6O_{10}][BO_3]Cl$	8.58	8.65	12.17	–	$Pca2_1$	(9)	–
1Δ6□	trembathite	[ϕ]⟨3□⟩|⟨3□⟩|⟨3□⟩|Δ	$Mg_3[B_6O_{10}][BO_3]Cl$	8.588(2)	8.588(2)	21.050(6)	–	$R3c$	(10)	–
4□	boracite (high)	[ϕ]□|□|□|□	$Mg_3[B_7O_{13}]Cl$	12.0986(2)	*a*	*a*	–	$F\bar{4}3c$	(11)	–
7Δ8□	pringleite	⟨Δ□•⟩=⟨Δ2□⟩Δ	$Ca_9[B_{20}O_{28}(OH)_{16}][B_6O_6(OH)_6]Cl_4(H_2O)_{13}$	12.746(2)	13.019(3)	9.693(2)	102.1(2)	$P1$	(12)	19d
7Δ8□	ruitenbergite	⟨Δ□•⟩=⟨Δ2□⟩Δ	$Ca_9[B_{20}O_{28}(OH)_{16}][B_6O_6(OH)_6]Cl_4(H_2O)_{13}$	19.857(7)	9.708(4)	17.522(6)	114.68(3)	$P2_1$	(12)	–
8Δ8□	penobsquisite	<Δ□•>=<Δ2□>–<Δ2□>$Ca_2Fe[B_9O_{13}(OH)_8]Cl(H_2O)_4$		11.63(4)	9.38(1)	8.735(9)	98.40(7)	$P2_1$	(13)	19e

metaborite: α=92.58°, γ=119.83°; hilgardite-1A: α=61.60(1)°, γ=105.86(1)°; hilgardite-3A: α=60.77(1)°, γ=83.96(1)°; tyretskite-1A: α = 61.8°, γ = 73.5°; pringleite: α=102.2(2)°, γ=85.6(1)°

(1) Zachariasen (1963), (2) Krogh-Moe (1962), (3) Burns & Hawthorne (1994d), (4) Ghose & Wan (1979), (5) Wan & Ghose (1983), (6) Kondrat'eva (1964), Ghose (1985), (7) Wendling *et al.* (1972), (8) Honea & Beck (1962), (9) Kühn & Schaacke (1955), (10) Burns *et al.* (1992), Schindler & Hawthorne (1998), (11) Sueno *et al.* (1973), (12) Grice *et al.* (1994), (13) Grice *et al.* (1996)

structure of nifontovite, and in decorated form in the structure of uralborite. The structure of metaborite is a simple $^{[4]}T\phi_2$ framework in which the B is [4]-coordinated and the anions are [2]-coordinated. However, there is extensive hydrogen bonding present that provides further linkage between the framework anions and that satisfies their local bond-valence requirements.

FBB = 2Δ2□:<Δ2□>=<Δ2□>

Diomignite, $Li_2B_4O_7$, is a rare anhydrous borate that has only been identified as a daughter mineral in a fluid inclusion in spodumene (London *et al.* 1987). The structure of diomignite contains the *FBB* 2Δ2□:<Δ2□>=<Δ2□> (Fig. 18b), which also occurs in a hydrated form in the finite-cluster minerals borax, tincalconite, hungchaoite, fedorovskite and roweite. The energetics of borate clusters with the general form 4B:<3B>=<3B> were investigated by Burns (1995); the 2Δ2□:<Δ2□>=<Δ2□> *FBB* was found to be the most stable owing to local bonding constraints. In the structure of diomignite, the *FBB*s polymerize such that each ($B\phi_3$) group shares an anion with a ($B\phi_4$) group of an adjacent *FBB*, resulting in a framework structure that is composed of two interlocking networks of polmerized *FBB*s (Fig. 19a). Additional bond-valence requirements of the anions are met by bonds to Li cations, which occur coordinated by six anions in voids in the framework.

FBB = 2Δ3□:<Δ2□>–<Δ2□>

Four minerals contain this *FBB*, the three polymorphs of hilgardite, $Ca_2[B_5O_9]Cl(H_2O)$, and tyretskite, $Ca_2[B_5O_9]OH(H_2O)$, which is isostructural with hilgardite-1A. The borate *FBB* (Fig. 18c) is anhydrous in all four structures, in which it occurs in two distinct stereo-isomers. Note that hydrated versions of this *FBB* occur in the structures of ulexite, probertite and tuzlaite. The structures of the hilgardite polymorphs and tyretskite consist of open zeolite-like borate frameworks, with Cl and OH^- anions and H_2O groups occurring in open channels in the structures (Fig. 19b). A detailed discussion of the stereochemistry of these structures is given by Ghose (1982). In brief, the *FBB*s link by sharing ($B\phi_4$) corners to form chains that extend along the *c* axis; each chain connects to adjacent chains by sharing corners between a ($B\phi_3$) group of one chain and a ($B\phi_4$) group of the adjacent chain. This connectivity results in a framework structure with open channels parallel to the *a*, *b* and *c* axis, with channel diameters of up to ~6 Å (Ghose & Wan 1979). The frameworks of the three polymorphs of hilgardite are distinct in the orientation of the ($B\phi_3$) groups along the *a* and *b* axes; otherwise, the frameworks are very similar.

FBB = 4□:[ϕ] □ | □ | □ | □
and Δ6□:[ϕ]<3□> | <3□> | <3□> | Δ

Boracite-group minerals are the naturally occurring subset of the boracite-type phases that have the general formula $M_3B_7O_{13}X$, where *M* is a divalent metal (Mg, Cr, Mn, Fe, Co, Ni, Cu, Zn, Cd), and *X* is a halogen atom (Cl, Br, I). Boracite-type phases have been prepared synthetically and extensively studied, owing to the ferroelastic, ferroelectric and magnetic properties of the crystals (*e.g.*, Nelmes 1974, Schmid & Tippmann 1978,

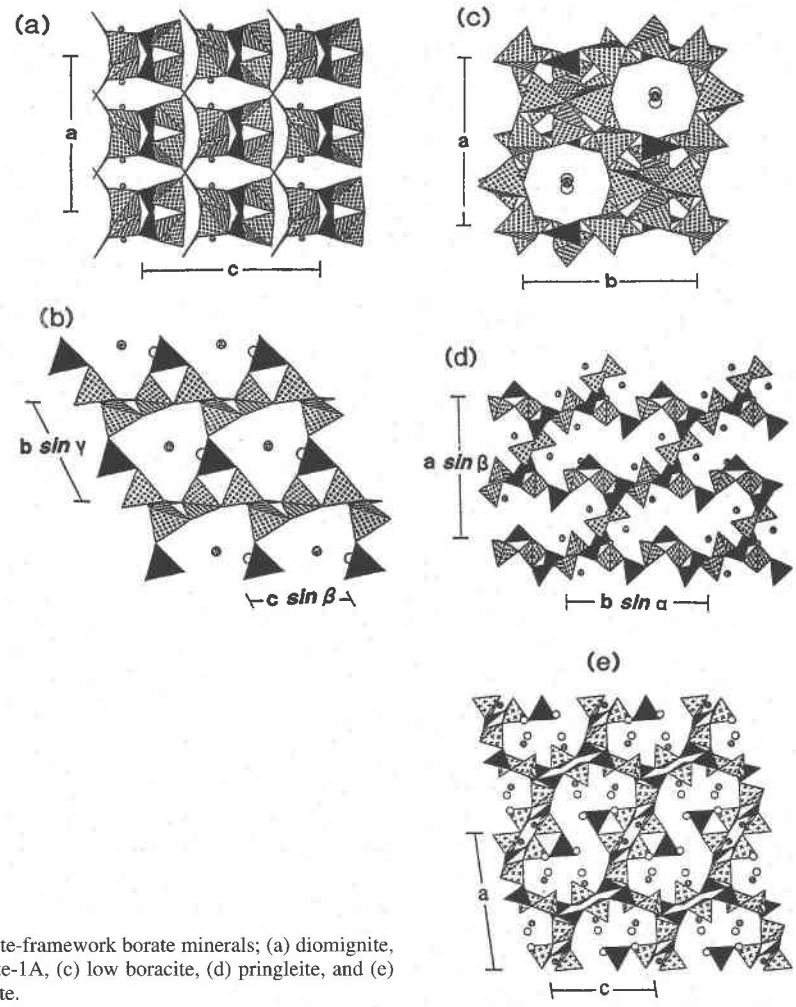

FIG. 19. Infinite-framework borate minerals; (a) diomignite, (b) hilgardite-1A, (c) low boracite, (d) pringleite, and (e) penobsquisite.

Tolédano *et al.* 1985, Moopenn & Coleman 1990, Crottaz *et al.* 1995). There are five boracite-group minerals; all contain Cl as the halogen, and the divalent metals are Mg, Fe and Mn.

The four boracite-group minerals boracite, $Mg_3B_7O_{13}Cl$, trembathite, $(Mg,Fe)_3B_7O_{13}Cl$, congolite, $(Fe,Mg)_3B_7O_{13}Cl$, and ericaite, $(Fe,Mg)_3B_7O_{13}Cl$, are each members of a complete $Mg_3B_7O_{13}Cl$–$Fe_3B_7O_{13}Cl$ solid-solution series. Chambersite, $Mn_3B_7O_{13}Cl$, is the fifth boracite-group mineral. Only very limited solid-solution occurs between chambersite and the Mg–Fe boracite-group minerals. Boracite, ericaite and chambersite have structures with orthorhombic symmetry (space group $Pca2_1$), whereas the structures of trembathite and congolite have rhombohedral symmetry (space group $R3c$). The phase relations in the series boracite – trembathite – congolite have been reported by Burns & Carpenter (1996) (Fig. 20). At 25°C, the orthorhombic boracite structure ($Pca2_1$) is stable for compositions from $Mg_3B_7O_{13}Cl$ to $Mg_{1.9}Fe_{1.1}B_7O_{13}Cl$, and the rhombohedral congolite structure ($R3c$) occurs for compositions ranging from $Mg_{1.9}Fe_{1.1}B_7O_{13}Cl$ to $Fe_3B_7O_{13}Cl$. Ericaite (Fe > Mg, $Pca2_1$) does not occur at room temperature.

The crystal structures of all boracite-group minerals have cubic symmetry (space group $F3c$) at high temperature (Burns & Carpenter 1996, 1997). The structure of cubic boracite (Ito *et al.* 1951, Sueno *et al.* 1973) consists of a framework of corner-sharing BO_4 tetrahedra, with the metal and halogen atoms located within cavities in the borate framework. The *FBB* for this structure is 4□:[ϕ] □ | □ | □ | □ |, indicating that a central oxygen atom is connected to four BO_4 tetrahedra (Fig. 18e). This situation is very unusual; cubic boracite is the only known structure that contains an oxygen atom [O(1) using the notation of Sueno *et al.* 1973] that is

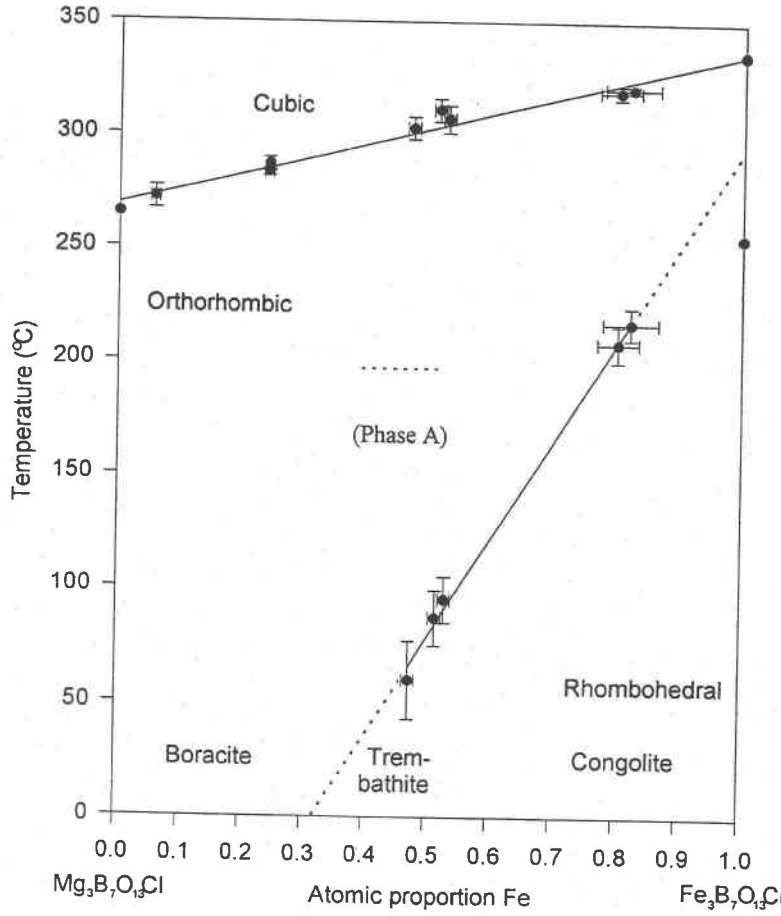

FIG. 20. The stability of the boracite – trembathite – congolite series as a function of temperature (from Burns & Carpenter 1996).

bonded to four boron atoms. The O(1) atom is located on a site with 23 point symmetry, and in cubic boracite each of the four *B*(3)–O(1) bond-lengths is 1.693(5) Å (Sueno *et al.* 1973), a value considerably longer than $<^{[4]}B–O> = 1.476$ Å found in minerals (Hawthorne *et al.* 1996). Significant anisotropic thermal motion of the *B*(3) and O(1) atoms, most likely about single potential-energy minima, is observed by diffraction techniques. An infrared spectroscopic study of crystals in the series $Mg_3B_7O_{13}Cl$–$Fe_3B_7O_{13}Cl$ suggests that there are BO_3 triangles locally present in the structure (Burns & Carpenter 1997), in contrast to the long-range structure obtained using diffraction techniques. The metal site is coordinated by six ligands; four equidistant equatorial oxygen atoms and two equidistant halogen atoms in a *trans* arrangement.

For all boracite-group minerals, cooling of the cubic structure results in a phase transition, or a series of phase transitions, to a structure with lower symmetry (Fig. 20). Evidence that crystals have undergone these phase transitions may be present as transformation-induced twins and anomalous optical properties. In the low-temperature structures, the O(1) position is bonded to three boron atoms only, and the borate framework contains both BO_4 tetrahedra and BO_3 triangles (Fig. 18d). The borate *FBB* of both the $Pca2_1$ and *R*3*c* structures is $\Delta 6\square:[\phi]<3\square> \mid <3\square> \mid <3\square> \mid \Delta$ (Fig. 19c). The $Pca2_1$ and *R*3*c* structures contain three and one symmetry-distinct metal sites, respectively. In each case, the coordination geometry of the cation is significantly distorted from the arrangement of the cubic structure.

$$FBB = 7\Delta 8\square:<\Delta\square\bullet>=<\Delta 2\square>\Delta$$

Pringleite and ruitenbergite are dimorphs of $Ca_9[B_{20}O_{28}(OH)_{18}][B_6O_6(OH)_6Cl_4(H_2O)_{13}$; together with penobsquisite (below), these borates display a new level of structural complexity in borate minerals. These

structures have borate frameworks that are remarkably open and that resemble aluminosilicate zeolites, raising the possibility of using borates in technological applications. To date, these extraordinary zeolite-like borates are only known from the marine-evaporite-hosted borate deposits of Sussex, New Brunswick (Roberts *et al.* 1993, Grice *et al.* 1996).

The structures of pringleite and ruitenbergite are closely related; each contains the unusually large *FBB* 7Δ8□:<Δ□Δ□Δ□Δ□Δ□Δ□Δ□ >=<Δ2□>Δ (abbreviated 7Δ8□:<Δ□•> = <Δ2□>Δ). The *FBB* contains a 12-membered ring of alternating ($B\phi_3$) and ($B\phi_4$) groups that share corners, with one of the ($B\phi_4$) tetrahedra also a component of a <Δ2□> ring that is in turn decorated with a single ($B\phi_3$) group (Fig. 18f). These large *FBB*s are connected by sharing corners through the <Δ2□>Δ component of the *FBB*, resulting in an open framework with channels along *c* and [110] (Fig. 19d) (Grice *et al.* 1994). The Ca cations are located in these channels, along with Cl^- anions and H_2O groups. Of these, some H_2O groups bond directly to Ca, others are only connected to the structure through hydrogen bonds. Each of the Cl^- anions is held in place in the channels by hydrogen bonds only. The distinction between pringleite and ruitenbergite involves subtle variations in the mode of polymerization of the *FBB*s (Grice *et al.* 1994).

FBB = *8Δ8□:<Δ□•> = <Δ2□>–<Δ2□>*

Penobsquisite, $Ca_2Fe[B_9O_{13}(OH)_6]Cl(H_2O)_4$, is the third zeolite-like borate to be discovered from the marine-evaporite-hosted borate deposits in Sussex, New Brunswick; the others are pringleite and ruitenbergite (above). The structure of penobsquisite contains the *FBB* 8Δ8□:<Δ□Δ□Δ□Δ□Δ□Δ□Δ□> – <Δ2□>–<Δ2□> (Grice *et al.* 1996). The *FBB* 6Δ6□:<Δ□•> is a twelve-membered ring of alternating, corner-sharing ($B\phi_3$) and ($B\phi_4$) groups (Fig. 18g), and also occurs as a component of the larger *FBB* of the structures of pringleite and ruitenbergite. In the penobsquisite structure, the 6Δ6□:<Δ□•> are connected to form sheets of 12-membered rings parallel to (100) at height *a*/2, whereas the 2Δ3□:<Δ2□>–<Δ2□> *FBB*s share corners to form crankshaft chains along *c* at height *a* = 0 (Fig. 19e). The sharing of corners between the layer of 6Δ6□:<Δ□•> at *a*/2 and the chains of 2Δ3□:<Δ2□>–<Δ2□> at height *a* = 0 results in an open, zeolite-like framework. The Ca and Fe cations occur in channels in the borate framework, the single Cl^- anion bonds to Fe and accepts hydrogen bonds, some H_2O groups are bonded to Ca or Fe, and two H_2O groups are only hydrogen-bonded in the structure.

Summary

Ninety-eight borate minerals have been arranged in a structural hierarchy based on the characteristics of polymerization of their constituent (BO_3) and (BO_4) tetrahedra. There is a tendency for structure types to adopt a simple pattern of polymerization, and there is only significant isotypism among minerals based on isolated (BO_3) and (BO_4) groups. The hierarchy developed here should be of importance in interpreting the chemical and paragenetic features of borate minerals.

Acknowledgements

We thank Lee Groat, Friedrick Liebau, Hugo Strunz, Associate Editor John Hughes and Editor Bob Martin for their comments on this manuscript. The work was supported by a Natural Sciences and Engineering Research Council of Canada Operating Grant to FCH and an NSERC Post-Doctoral Fellowship to PCB.

References

Alfredsson, V., Bovin, J.-O., Norrestam, R. & Terasaki, O. (1991): The structure of the mineral chestermanite, $Mg_{2.25}Al_{0.16}Fe_{0.43}Ti_{0.02}Sb_{0.13}O_2BO_3$. A combined single-crystal X-ray and HREM study. *Acta Chem. Scand.* **45**, 797-804.

Behm, H. (1983): Hexasodium (*cyclo*-decahydroxotetracosaoxohexadecaborato)dicuprate(II) dodecahydrate, $Na_6[Cu_2\{B_{16}O_{24}(OH)_{10}\}]\cdot 12H_2O$. *Acta Crystallogr.* **C39**, 20-22.

_____ (1985): Hexapotassium (*cyclo*-octahydroxotetracosaoxohexadecaborato) dioxouranate(VI) dodecahydrate, $K_6[UO_2\{B_{16}O_{24}(OH)_8\}]\cdot 12H_2O$. *Acta Crystallogr.* **C41**, 642-645.

Bermanec, V., Armbruster, T., Tibljas, D., Sturman, D. & Kniewald, G. (1994): Tuzlaite, $NaCa[B_5O_8(OH)_2]\cdot 3H_2O$, a new mineral with a pentaborate sheet structure from the Tuzla salt mine, Bosnia and Hercegovina. *Am. Mineral.* **79**, 562-569.

Bigi, S., Brigatti, M.F. & Capedri, S. (1991): Crystal chemistry of Fe- and Cr-rich warwickite. *Am. Mineral.* **76**, 1380-1388.

Bonazzi, P. & Menchetti, S. (1989): Contribution to the crystal chemistry of the minerals of the ludwigite–vonsenite series. *Neues Jahrb. Mineral., Monatsh.*, 69-83.

_____, _____, Sabelli, C. & Trosti-Ferroni, R. (1986): Karlite: crystal structure and chemical composition. *Neues Jahrb. Mineral., Monatsh.*, 253-262.

Bondareva, O.F., Simonov, M.A. & Belov, N.V. (1978): The crystal structure of synthetic jimboite $Mn_3(BO_3)_2$. *Sov. Phys. Crystallogr.* **23**, 272-273.

Bovin, J.-O., Carlsson, A., Sjövall, R., Thomasson, R., Norrestam, R. & Søtofte, I. (1996): The crystal structure of a blatterite mineral, $Mg_{1.33}Mn_{1.44}Fe_{0.05}Sb_{0.17}O_2BO_3$, a combined single crystal X-ray and HREM study. *Z. Kristallogr.* **211**, 440-448.

BROVKIN, A.A., ZAYAKINA, N.V. & BROVKINA, V.S. (1975): Crystal structure of strontioborite $Sr[B_8O_{11}(OH)_4]$. *Sov. Phys. Crystallogr.* **20**, 563-566.

BROWN, G.E. & CLARK, J.R. (1978): Crystal structure of hydrochlorborite, $Ca_2[B_3O_3(OH)_4{\bullet}OB(OH)_3]Cl{\bullet}7H_2O$, a seasonal evaporite mineral. *Am. Mineral.* **63**, 814-823.

BURNS, P.C. (1995): Borate clusters and fundamental building blocks containing four polyhedra: why few clusters are utilized as fundamental building blocks of structures. *Can. Mineral.* **33**, 1167-1176.

_____ & CARPENTER, M.A. (1996): Phase transitions in the series boracite – trembathite – congolite: phase relations. *Can. Mineral.* **34**, 881-892.

_____ & _____ (1997): Phase transitions in the series boracite – trembathite – congolite: an infrared spectroscopic study. *Can. Mineral.* **36**, 189-202.

_____, COOPER, M.A. & HAWTHORNE, F.C. (1994): Jahn–Teller-distorted $Mn^{3+}O_6$ octahedra in fredrikssonite, the fourth polymorph of $Mg_2Mn^{3+}(BO_3)O_2$. *Can. Mineral.* **32**, 397-403.

_____, GRICE, J.D. & HAWTHORNE, F.C. (1995): Borate minerals. I. Polyhedral clusters and fundamental building blocks. *Can. Mineral.* **33**, 1131-1151.

_____ & HAWTHORNE, F.C. (1993a): Hydrogen bonding in colemanite, an X-ray and structure energy study. *Can. Mineral.* **31**, 297-304.

_____ & _____ (1993b): Hydrogen bonding in meyerhofferite, an X-ray and structure energy study. *Can. Mineral.* **31**, 305-312.

_____ & _____ (1994a): Hydrogen bonding in tunellite. *Can. Mineral.* **32**, 895-902.

_____ & _____ (1994b): Structure and hydrogen bonding in preobrazhenskite, a complex heteropolyhedral borate. *Can. Mineral.* **32**, 387-396.

_____ & _____ (1994c): Structure and hydrogen bonding in inderborite, a heteropolyhedral sheet structure. *Can. Mineral.* **32**, 533-539.

_____ & _____ (1994d): Refinement of the structure of hilgardite-1A. *Acta Crystallogr.* **C50**, 653-655.

_____ & _____ (1994e): Kaliborite: an example of a crystallographically symmetrical hydrogen bond. *Can. Mineral.* **32**, 885-894.

_____, _____ & STIRLING, J.A.R. (1992): Trembathite, $(Mg,Fe)_3B_7O_{13}Cl$, a new borate mineral from the Salt Springs potash deposit, Sussex, New Brunswick. *Can. Mineral.* **30**, 445-448.

CANNILLO, E., DAL NEGRO, A. & UNGARETTI, L. (1973): The crystal structure of ezcurrite. *Am. Mineral.* **58**, 110-115.

CHRIST, C.L. (1960): Crystal chemistry and systematic classification of hydrated borate minerals. *Am. Mineral.* **45**, 334-340.

_____ & CLARK, J.R. (1977): A crystal-chemical classification of borate structures with emphasis on hydrated borates. *Phys. Chem. Minerals* **2**, 59-87.

_____ & GARRELS, R.M. (1959): Relations among sodium borate hydrates at the Kramer deposit, Boron, California. *Am. J. Sci.* **257**, 516-528.

CLARK, J.R., APPLEMAN, D.E. & CHRIST, C.L. (1964): Crystal chemistry and structure refinement of five hydrated calcium borates. *J. Inorg. Nucl. Chem.* **26**, 73-95.

_____ & CHRIST, C.L. (1971): Veatchite: crystal structure and correlations with p-veatchite. *Am. Mineral.* **56**, 1934-1954.

COLLIN, R.L. (1951): The crystal structure of bandylite, $CuCl_2{\bullet}CuB_2O_4{\bullet}4H_2O$. *Acta Crystallogr.* **4**, 204-209.

COOPER, M.A. & HAWTHORNE, F.C. (1998): The crystal structure of blatterite, $Sb^{5+}{}_3Mn^{3+}{}_9$ $(Mn^{2+},Mg)_{35}(BO_3)_{16}O_{32}$, and structural hierarchy in the zigzag borates. *Can. Mineral.* **37**, 1171-1193.

_____, _____, NOVÁK, M. & TAYLOR, M.C. (1994): The crystal structure of tusionite, $Mn^{2+}Sn^{4+}(BO_3)_2$, a dolomite-structure borate. *Can. Mineral.* **32**, 903-908.

COOPER, W.F., LARSEN, F.K., COPPENS, P. & GIESE, R.F. (1973): Electron population analysis of accurate diffraction data. V. Structure and one-center charge refinement of the light-atom mineral kernite, $Na_2B_4O_6(OH)_2{\bullet}3H_2O$. *Am. Mineral.* **58**, 21-31.

CORAZZA, E. (1974): The crystal structure of kurnakovite: a refinement. *Acta Crystallogr.* **B30**, 2194-2199.

_____ (1976): Inderite: crystal structure refinement and relationship with kurnakovite. *Acta Crystallogr.* **B32**, 1329-1333.

_____, MENCHETTI, S. & SABELLI, C. (1974): The crystal structure of biringuccite, $Na_4[B_{10}O_{16}(OH)_2]{\bullet}2H_2O$. *Am. Mineral.* **59**, 1005-1015.

_____, _____ & _____ (1975): The crystal structure of nasinite, $Na_2[B_5O_8(OH)]{\bullet}2H_2O$. *Acta Crystallogr.* **B31**, 2405-2410.

CROTTAZ, O., KUBEL, F. & SCHMID, H. (1995): High-temperature single-crystal X-ray-diffraction-structure of cubic manganese iodine and manganese bromine boracites. *J. Solid State Chem.* **120**, 60- 63.

DAL NEGRO, A., MARTIN POZAS, J.M. & UNGARETTI, L. (1975): The crystal structure of ameghinite. *Am. Mineral.* **60**, 879-883.

_____, SABELLI, C. & UNGARETTI, L. (1969): The crystal structure of mcallisterite, $Mg_2[B_6O_7(OH)_6]_2{\bullet}9H_2O$. *Atti*

Accad. Naz. Lincei, Classe di Scienze Fisiche, Matematiche e Naturali, Rendiconti **XLVII**, 353-364.

_____ & TADINI, C. (1974): Refinement of the crystal structure of fluoborite, $Mg_3(F,OH)_3(BO_3)$. *Tschermaks Mineral. Petrogr. Mitt.* **21**, 94-100.

_____, UNGARETTI, L. & SABELLI, C. (1971): The crystal structure of aksaite. *Am. Mineral.* **56**, 1553-1566.

_____, _____ & _____ (1973): Crystal structure of rivadavite. *Naturwissen.* **60**, 350.

DE WAAL, S.A., VILJOEN, E.A. & CALK, L.C. (1974): Nickel minerals from Barberton, South Africa. VII. Bonaccordite, the nickel analogue of ludwigite. *Trans. Geol. Soc. S. Africa* **77**, 375.

DOWTY, E. & CLARK, J.R. (1973): Crystal-structure refinements for orthorhombic boracite, $Mg_3ClB_7O_{13}$, and a trigonal, iron-rich analogue. *Z. Kristallogr.* **138**, 64-99.

EDWARDS, J.O. & ROSS, V.F. (1960): Structural principles of the hydrated polyborates. *J. Inorg. Nucl. Chem.* **15**, 329-337.

EFFENBERGER, H. (1982): Verfeinerung der Kristallstruktur von synthetischem Teepleit. *Acta Crystallogr.* **B38**, 82-85.

_____ & PERTLIK, F. (1984): Verfeinerung der Kristallstrukturen der isotypen verbindungen $M_3(BO_3)_2$ mit M = Mg, Co, Ni (Structurtyp: Kotoit). *Z. Kristallogr.* **166**, 129-140.

_____ & ZEMANN, J. (1986): The detailed crystal structure of nordenskiöldine, $CaSn(BO_3)_2$. *Neues Jahrb. Mineral., Monatsh.*, 111-114.

EGOROV-TISMENKO, Y.K., SIMONOV, M.A. & BELOV, N.V. (1980): Crystal structures of calciborite $Ca_2[BO_3BO]_2$ and synthetic calciboraluminate $2CaAl[BO_3] \equiv Ca_2[AlO_3BO]_2$. *Sov. Phys. Dokl.* **25**, 226-227.

ERD, R.C., MCALLISTER, J.F. & VLISIDIS, A.C. (1961): Nobleite, another new hydrous calcium borate from the Death Valley region, California. *Am. Mineral.* **46**, 560-571.

FANG, J.H. & NEWNHAM, R.E. (1965): The crystal structure of sinhalite. *Mineral. Mag.* **35**, 196-199.

GENKINA, E.A. & MALINOVSKII, YA.A. (1983): Refinement of the structure of pinnoite: location of hydrogen atoms. *Sov. Phys. Crystallogr.* **28**, 475-477.

GHOSE, S. (1982): Stereoisomerism of the pentaborate polyanion $[B_5O_{12}]^{9-}$, polymorphism and piezoelectricity in the hilgardite groups of minerals: a novel class of polar borate zeolites. *Am. Mineral.* **67**, 1265-1272.

_____ (1985): A new nomenclature for the borate minerals in the hilgardite ($Ca_2B_5O_9Cl{\bullet}H_2O$) – tyretskite ($Ca_2B_5O_9OH{\bullet}H_2O$) group. *Am. Mineral.* **70**, 636-637.

_____ & WAN, CHE'NG (1977): Aristarainite: $Na_2Mg[B_6O_8(OH)_4]_2{\bullet}4H_2O$: a sheet structure with chains of hexaborate polyanions. *Am. Mineral.* **62**, 979-989.

_____ & _____ (1979): Hilgardite, $Ca_2[B_5O_9]Cl{\bullet}H_2O$: a piezoelectric zeolite-type pentaborate. *Am. Mineral.* **64**, 187-195.

_____, _____ & CLARK, J.R. (1978): Ulexite, $NaCaB_5O_6(OH)_6{\bullet}5H_2O$: structure refinement, polyanion configuration, hydrogen bonding, and fiber optics. *Am. Mineral.* **63**, 160-171.

GRICE, J.D., BURNS, P.C. & HAWTHORNE, F.C. (1994): Determination of the megastructures of the borate polymorphs pringleite and ruitenbergite. *Can. Mineral.* **32**, 1-14.

_____, GAULT, R.A. & VAN VELTHUIZEN, J. (1996): Penobsquisite: a new borate mineral with a complex framework structure. *Can. Mineral.* **34**, 657-665.

_____, _____ & _____ (1997): Brianroulstonite: a new borate mineral with a sheet structure. *Can. Mineral.* **35**, 751-758.

HAWTHORNE, F.C. (1983): Graphical enumeration of polyhedral clusters. *Acta Crystallogr.* **A39**, 724- 736.

_____ (1985): Towards a structural classification of minerals: the $^{vi}M^{iv}T_2\phi_n$ minerals. *Am. Mineral.* **70**, 455-473.

_____ (1986): Structural hierarchy in $^{VI}M_x^{III}T_y\phi_z$ minerals. *Can. Mineral.* **24**, 625-642.

_____ (1990): Structural hierarchy in $M^{[6]}T^{[4]}\phi_n$ minerals. *Z. Kristallogr.* **192**, 1-52.

_____ (1994): Structural aspects of oxide and oxysalt crystals. *Acta Crystallogr.* **B50**, 481-510.

_____, BURNS, P.C. & GRICE, J.D. (1996): The crystal chemistry of boron. *In* Boron: Mineralogy, Petrology and Geochemistry (E.S. Grew & L.M. Anovitz, eds.). *Rev. Mineral.* **33**, 41-115.

HELLER, G. (1970): Darstellung und Systematisierung von Boraten und Polyboraten. *Fortschr. Chem. Forsch.* **15**, 206-280.

_____ & PICKARDT, J. (1985): Über ein Ikosaborat-ion in hydratisierten Kalium- und Natriumkupferpolyboraten. *Z. Naturforsch.* **40b**, 462-466.

HOFFMANN, C. & ARMBRUSTER, T. (1995): Crystal structure of a (001) twinned sussexite $Mn_2B_2O_4(OH)_2$ from the Kalahari Manganese Field, South Africa. *Schweiz. Mineral. Petrogr. Mitt.* **75**, 123-133.

HONEA, R.M. & BECK, F.R. (1962): Chambersite, a new mineral. *Am. Mineral.* **47**, 665-671.

HOTOKKA, M. & PYYKKÖ, P. (1989): An ab initio study of bonding trends in the series BO_3^{3-}, CO_3^{2-}, NO_3^- and O_4 (D_{3h}). *Chem. Phys. Lett.* **157**, 415-418.

HUANG, ZOULIANG & WANG, PU (1994): Yuanfuliite – a new borate mineral. *Acta Petrol. Mineral.* **13**, 328-334 (in Chinese, Engish abstr.).

ITO, T., MORIMOTO, N. & SADANAGA, R. (1951): The crystal structure of boracite. *Acta Crystallogr.* **4**, 310-316.

KAZANSKAYA, E.V., CHEMODINA, T.N., EGOROV-TISMENKO, Y.K., SIMONOV, M.A. & BELOV, N.V. (1977): Refined crystal structure of pentahydroborite $Ca[B_2O(OH)_6]\cdot 2H_2O$. *Sov. Phys. Crystallogr.* **22**, 35-36.

KONDRAT'EVA, V.V. (1964): X-ray study of some minerals of the hilgardite group. *In* X-Ray Studies on Mineral Raw Materials **4**. Nedra, Moscow, Russia (10-18).

KONEV, A.A., LEBEDEVA, V.S., KASHAEV, A.A. & USHCHAPOVSKAYA, Z.F. (1970): Azoproite, a new mineral of the ludgwigite group. *Zap. Vses. Mineral. Obshchest.* **99**, 225-231 (in Russ.).

KONNERT, J.A., CLARK, J.R. & CHRIST, C.L. (1970a): Crystal structure of strontioginorite, $(Sr,Ca)_2B_{14}O_{20}(OH)_6\cdot 5H_2O$. *Am. Mineral.* **55**, 1911-1931.

_____, _____ & _____ (1970b): Crystal structure of fabianite, $CaB_3O_5(OH)$, and comparison with the structure of its synthetic dimorph. *Z. Kristallogr.* **132**, 241-254.

_____, _____ & _____ (1972): Gowerite, $CaB_5O_8(OH)\cdot B(OH)_3\cdot 3H_2O$: crystal structure and comparison with related borates. *Am. Mineral.* **57**, 381-396.

KROGH-MOE, J. (1962): The crystal structure of lithium diborate, $Li_2O\cdot 2B_2O_3$. *Acta Crystallogr.* **15**, 190-193.

KÜHN, R. & SCHAACKE, I. (1955): Vorkommen und Analyse der Boracit- und Ericaitkrystalle aus dem Salzhorst von Wathlingen-Hanigsen. *Kali und Steinsalz* **11**, 33-42.

LEVY, H.A. & LISENSKY, G.C. (1978): Crystal structures of sodium sulfate decahydrate (Glauber's salt) and sodium tetraborate decahydrate (borax). Redetermination by neutron diffraction. *Acta Crystallogr.* **B34**, 3502-3510.

LONDON, D., ZOLENSKY, M.E. & ROEDDER, E. (1987): Diomignite: natural $Li_2B_4O_7$ from the Tanco pegmatite, Bernic Lake, Manitoba. *Can. Mineral.* **25**, 173-180.

MALINKO, S.V., SHASHKIN, D.P. & YURKINA, K.V. (1976): Fedorovskite, a new boron mineral, and the isomorphous series roweite – fedorovskite. *Zap. Vses. Mineral. Obshchest.* **105**, 71-85 (in Russ.).

MANDARINO, J.A., RACHLIN, A.L., DUNN, P.J., LE PAGE, Y., BACK, M.E., MUROWCHICK, B.L., RAMIK, R.A. & FALLS, R.B. (1990): Redefinition of volkovskite and its description from Sussex, New Brunswick. *Can. Mineral.* **28**, 351-356.

MENCHETTI, S., SABELLI, C. & TROSTI-FERRONI, R. (1982): Probertite, $CaNa[B_5O_7(OH)_4]\cdot 3H_2O$: a refinement. *Acta Crystallogr.* **B38**, 3072-3075.

MERLINO, S. & SARTORI, F. (1969): The crystal structure of larderellite, $NH_4B_5O_7(OH)_2\cdot H_2O$. *Acta Crystallogr.* **B25**, 2264-2270.

_____ & _____ (1971): Ammonioborite: new borate polyion and its structure. *Science* **171**, 377-379.

_____ & _____ (1972): The crystal structure of sborgite, $NaB_5O_6(OH)_4\cdot 3H_2O$. *Acta Crystallogr.* **B28**, 3559-3567.

MOOPENN, A. & COLEMAN, L.B. (1990): Vibrational spectroscopy and the improper phase transition in nickel bromide and copper chloride boracite. *J. Phys. Chem. Solids* **51**, 1099-1110.

MOORE, P.B. & ARAKI, T. (1972a): Wightmanite, $Mg_5(O)(OH)_5[BO_3]\cdot nH_2O$, a natural drainpipe. *Nature Phys. Sci.* **239**, 25-26.

_____ & _____ (1972b): Johachidolite, $CaAl[B_3O_7]$, a borate with very dense atomic structure. *Nature Phys. Sci.* **240**, 63-65.

_____ & _____ (1974a): Pinakiolite, $Mg_2Mn^{3+}O_2[BO_3]$; warwickite, $Mg(Mg_{0.5}Ti_{0.5})O[BO_3]$; wightmanite, $Mg_5(O)(OH)_5[BO_3]\cdot nH_2O$: crystal chemistry of complex 3 Å wallpaper structures. *Am. Mineral.* **59**, 985-1004.

_____ & _____ (1974b): Roweite, $Ca_2Mn^{2+}{}_2(OH)_4[B_4O_7(OH)_2]$: its atomic arrangement. *Am. Mineral.* **59**, 60-65.

_____ & _____ (1976): Painite, $CaZrB[Al_9O_{18}]$: its crystal structure and relation to jeremejevite, $B_5[\square_3Al_6(OH)_3O_{15}]$, and fluoborite, $B_3[Mg_9(F,OH)_9O_9]$. *Am. Mineral.* **61**, 88-94.

NAKAI, I., OKADA, H., MASUTOMI, K., KOYAMA, E. & NAGASHIMA, K. (1986): Henmilite, $Ca_2Cu(OH)_4[B(OH)_4]_2$, a new mineral from Fuka, Okayama Prefecture, Japan. I. Occurrence and description. *Am. Mineral.* **71**, 1234-1239.

NELMES, R.J. (1974): Structural studies of boracites. A review of the properties of boracites. *J. Phys. C: Solid State Phys.* **7**, 3840-3854.

NORRESTAM, R. & BOVIN, J.-O. (1987): The crystal structure of takéuchiite, $Mg_{1.71}Mn_{1.29}BO_5$, a combined single crystal X-ray and HRTEM study. *Z. Kristallogr.* **181**, 135-149.

POWELL, D.R., GAINES, D.F., ZERELLA, P.J. & SMITH, R.A. (1991): Refinement of the structure of tincalconite. *Acta Crystallogr.* **C47**, 2279-2282.

RACHLIN, A.L., MANDARINO, J.A., MUROWCHICK, B.L., RAMIK, R.A., DUNN, P.J. & BACK, M.E. (1986): Mineralogy of hilgardite-4M from evaporites in New Brunswick. *Can. Mineral.* **24**, 689-693.

RASTSVETAEVA, R.K., ANDRIANOV, V.I., GENKINA, E.A., SOKOLOVA, T.N. & KASBAEV, A.A. (1992): Crystal structure of volkovskite. *Kristallografiya* **37**, 326-333 (in Russ.).

ROBERTS, A.C., STIRLING, J.A.R., GRICE, J.D., BURNS, P.C., ROULSTON, B.V., CURTIS, J.D. & JAMBOR, J.L. (1993): Pringleite and ruitenbergite, polymorphs of $Ca_9B_{26}O_{34}(OH)_{24}Cl_4\cdot 13H_2O$, two new mineral species from Sussex, New Brunswick. *Can. Mineral.* **31**, 795-800.

ROSS, V.F. & EDWARDS, J.O. (1967): The structural chemistry of the borates. *In* The Chemistry of Boron and its Compounds (E.L. Muetterties, ed.). John Wiley & Sons, New York, N.Y. (155-207).

ROULSTON, B.V. & WAUGH, D.C.E. (1981): A borate-mineral assemblage from the Penobsquis and Salt Springs evaporite deposits of southern New Brunswick. *Can. Mineral.* **19**, 291-301.

RUMANOVA, I.M. & GANDYMOV, O. (1971): The crystal structure of the natural strontium borate, p-veatchite, $Sr_2[B_5O_8(OH)]_2 \bullet B(OH)_3 \bullet H_2O$. *Sov. Phys. Crystallogr.* **16**, 75-81.

SABELLI, C. & STOPPIONI, A. (1978): Refinement of the structure of hydroboracite. *Can. Mineral.* **16**, 75-80.

SCHINDLER, M. & HAWTHORNE, F.C. (1998): The crystal structure of trembathite, $(Mg_{1.55}Fe_{1.43}Mn_{0.02})\ B_7O_{13}Cl$, a mineral of the boracite group: an example of the insertion of a cluster into a three-dimensional net. *Can. Mineral.* **36**, 1195-1201.

SCHMID, H. & TIPPMANN, H. (1978): Spontaneous birefringence in boracites – measurements and applications. *Ferroelectrics* **20**, 21-36.

SIMONOV, M.A., EGOROV-TISMENKO, YU.K. & BELOV, N.V. (1976c): Refined crystal structure of wimsite $Ca(B_2O_2(OH)_4)$. *Sov. Phys. Crystallogr.* **21**, 332-333.

_____, _____ & _____ (1977): Accurate crystal structure of uralborite, $Ca_2[B_4O_4(OH)_8]$. *Sov. Phys. Dokl.* **22**, 277-279.

_____, _____, KAZANSKAYA, E.V., BELOKONEVA, E.L. & BELOV, N.V. (1978): Hydrogen bonds in the crystal structure of nifontovite $Ca_2[B_5O_3(OH)_6]_2 \bullet 2H_2O$. *Sov. Phys. Dokl.* **23**, 159-161.

_____, _____, EGOROV-TISMENKO, YU.K., ZHELEZIN, E.P. & BELOV, N.V. (1976a): Refinement of the crystal structure of frolovite $Ca[B(OH)_4]_2$. *Sov. Phys. Dokl.* **21**, 471-473.

_____, YAMANOVA, N.A., KAZANSKAYA, E.V., EGOROV-TISMENKO, Y.K. & BELOV, N.V. (1976b): Crystal structure of a new natural calcium borate, hexahydroborite $CaB_2O_4 \bullet 6H_2O \equiv Ca[B(OH)]_2 \bullet 2H_2O$. *Sov. Phys. Dokl.* **21**, 314-316.

SOKOLOVA, E.V., EGOROV-TISMENKO, YU.K., KARGAL'TSEV, S.V., KLYAKHIN, V.A. & URUSOV, V.S. (1987): Refinement of the crystal structure of synthetic fluorian jeremejevite, $Al_6(BO_3)_3F_3$. *Vestn. Mosk. Univ. Geol.* **87**, 82-84 (in Russ.).

STRUNZ, H. (1997): Classification of borate minerals. *Eur. J. Mineral.* **9**, 225-232.

SUENO, S., CLARK, J.R., PAPIKE, J.J. & KONNERT, J.A. (1973): Crystal-structure refinement of cubic boracite. *Am. Mineral.* **58**, 691-697.

SWINNEA, J.S. & STEINFINK, H. (1983): Crystal structure and Mössbauer spectrum of vonsenite, $2FeO \bullet FeBO_3$. *Am. Mineral.* **68**, 827-832.

TAKÉUCHI, Y. (1952): The crystal structure of magnesium pyroborate. *Acta Crystallogr.* **5**, 574-581.

_____ (1978): "Tropochemical twinning": a mechanism of building complex structures. *Recent Prog. Nat. Sci. Japan* **3**, 153-182.

_____, HAGA, N., KATO, T. & MIURA, Y. (1978): Orthopinakiolite, $Mg_{2.95}O_2[BO_3]$: its crystal structure and relationship to pinakiolite, $Mg_{2.90}O_2[BO_3]$. *Can. Mineral.* **16**, 475-485.

_____ & KUDOH, Y. (1975): Szaibelyite, $Mg_2(OH)[B_2O_4(OH)]$: crystal structure, pseudosymmetry, and polymorphism. *Am. Mineral.* **60**, 273-279.

TENNYSON, C. (1963): Eine Systematik der Borate auf kristallchemischer Grundlage. *Fortschr. Mineral.* **41**, 64-91.

TOLÉDANO, P., SCHMID, H., CLIN, M. & RIVERA, J.P. (1985): Theory of the low-temperature phases in boracites: latent antiferromagnetism, weak ferromagnetism, and improper magnetostructural couplings. *Phys. Rev.* **32**, 6006-6039.

WAN, CH'ENG & GHOSE, S. (1977): Hungchaoite, $Mg(H_2O)_5\ B_4O_5(OH)_4 \bullet 2H_2O$: a hydrogen-bonded molecular complex. *Am. Mineral.* **62**, 1135-1143.

_____ & _____ (1983): Parahilgardite, $Ca_6[B_5O_9]_3\ Cl_3 \bullet 3H_2O$: a triclinic piezoelectric zeolite-type pentaborate. *Am. Mineral.* **68**, 604-613.

WENDLING, E., HODENBERG, R.V. & KÜHN, R. (1972): Congolit, der trigonale Eisenboracit. *Kali und Steinsalz* **6**, 1-3.

YAKUBOVICH, O.V., YAMNOVA, N.A., SHCHEDRIN, B.M., SIMONOV, M.A. & BELOV, N.V. (1976): The crystal structure of magnesium kurchatovite, $CaMg[B_2O_5]$. *Sov. Phys. Dokl.* **21**, 294-296.

YAMNOVA, N.A., SIMONOV, M.A. & BELOV, N.V. (1977): Refined crystal structure of solongoite $Ca_2[B_3O_4(OH)_4]Cl$. *Sov. Phys. Crystallogr.* **22**, 356-357.

_____, SIMONOV, M.A. & BELOV, N.V. (1978): The distribution of the cations Sn, Fe^{3+}, Fe^{2+}, Mg in the crystal structure of hulsite. *Dokl. Akad. Nauk SSSR* **238**, 1094-1097 (in Russ.).

YANG, GUANGMING, PENG, ZHIZHONG & PAN, ZHAOLU (1985): Magnesiohulsite – a new tin-rich borate mineral. *Acta Mineral. Sinica* **5**, 97-101 (in Chinese, with English abstr.).

ZACHARIASEN, W.H. (1963): The crystal structure of cubic metaboric acid. *Acta Crystallogr.* **16**, 380-384.

Received April 30, 1998, revised manuscript accepted January 29, 1999.